The optimal meander planform shape from minimization of entropy production

Frans Buschman

April 5, 2004

Summary

All over the world natural lowland rivers and streams are winding through the sediments deposited in earlier times. These meandering rivers and streams show remarkable geometric similarity: the ratio of the meander length to the width of the channel is constant. The process of meandering is thus independent of scale.

Many theories and models are proposed to explain the process of meandering, but still meandering is not completely understood, due to the complexity of the processes involved. The valley slope, bankfull discharge, sediment transported, vegetation growth, and bed material all influence the processes of meandering. Moreover they are rarely uniform and the conditions usually change with time, because of changing geology, climate or activities by man. Consequently, the sinuosity of a meandering channel is difficult to predict. To explain the behavior of meandering channels, Stølum [1996, 1998] proposed that meandering can be described with the self-organizing process: clusters of cut-offs of the meander planform tend to cause a transition from active meandering with many cut-off events into a stable, more ordered state without cut-offs. After some time, the channel may change into the active state, if a cluster of cut-offs happens at for example high discharges. In this way stabilized meandering channels with constant planform shape can be found in most natural river reaches, if sufficient time is present to adapt to the conditions. For a meandering river the timescale of the channel in stable state is likely to be hundreds of years.

In nature, these stabilized meandering channels show two asymmetries in their planform resulting from the interaction of flow and form: an upvalley skew of the meandering channel's minima and maxima and a delayed inflection point. Another planform characteristic is fattening with respect to a first order sine-generated curve. In this research attempts were made to derive this optimal planform shape given the sinuosity from minimization of entropy production. Entropy is constantly produced in an open channel by friction. Prigogine [1945] stated that linear thermodynamic systems close to equilibrium evolve toward a stationary state characterized by the minimum entropy production compatible with the constraints imposed on the system. This statement is extended by Reiser [1996, 1998] to be valid for open, non-linear systems like meandering channels as well.

The problem of finding the optimal meander planform shape is reformulated as an optimal control problem. In this problem the dimensionless Odgaard model is used to describe the flow in alluvial meandering channels. The optimal meander planform is calculated from minimization of total entropy production over one meander period. To find this optimal shape, the control or the curvature at the centerline is changed at every longitudinal location. At every

longitudinal point the states and entropy production are derived from this control by numerical integration. With this model, no assumptions are made about the planform shape and the channel is free to flow in the most efficient way. For a sinuosity of three, a result was obtained, which exhibits most typical characteristics of natural, alluvial meanders.

Preface

In May 2003 I started to explore the world of meandering. Soon it was clear for me that many theories based on different principles were proposed to understand the process of meandering. The processes are complex and not completely understood. It was a challenge to understand the different theories and to improve them. In the beginning of this study, I focused on the sinuosity of meandering rivers. It became clear that many factors influence this variable and a prediction seems to be very difficult. Then it came out that the article by Ryan Teuling, Schalk-Jan van Andel and Peter Troch submitted to water resources research was not accepted. In this article the meander planform is derived from an entropy principle. In my study a slightly different entropy principle was used. This was the result of three days of presentation and discussion with a thermodynamic expert: Bernard Reiser. The main reason for not accepting the article, was the assumption that prescribes the meander planform. Therefore we changed the focus of my research into the planform shape of alluvial meanders. I tried to find extra equations, which have to be satisfied for a stabilized meandering channel with minimal entropy production. These are Euler-Lagrange equations and we thought of ways to implement these into the calculation scheme of the article to circumvent the assumption about the planform shape. I tried to think of different numerical calculation schemes, but that was trying to repeat many years of developing variational methods. Luckily I came into contact with Gerard van Willigenburg, who is a variational methods expert of the systems and control group of the department Agrotechnology. The problem of finding the meander planform shape appeared to be an optimal control problem. We reformulated the problem and after many attempts one result showed the typical characteristics of natural, alluvial meandering channels.

This was my first thesis and I learned very much: not only about meandering, but also about writing a scientific report in English and about the ups and downs inherent to doing research. I am very thankful for the friendly, scientific atmosphere in the hydrology and quantitative water management group. Everybody is willing to help by answering questions and giving ideas. In the first place I would like to thank both my supervisors Peter Troch and Gerard van Willigenburg for their comments and suggestions and Ryan Teuling for always being ready for questions and sharing his ideas. Special thanks for the hydrology and quantitative water management group go to Paul Torfs, who was always present to solve mathematical problems with me, Patrick Bogaart, the geomorphologist and Hidde Leijnse, who helped me with LateX and matlab often. From outside the Wageningen University I would like to thank Bernard Reiser, Erik Mosselman (WL) and Koen Blanckaert.

List of symbols

a	constant in equation 3.10 that follows from AIV-4		$-$
a'	constant described in AIII-3a		$-$
b	constant in equation 3.10 that follows from AIV-4		$-$
b'	constant described in AIII-3b		$-$
c	curvature		m^{-1}
c'	constant described in AIII-3c		$-$
C	Chézy coefficient		$m^{0.5}s^{-1}$
c_c	curvature at the centerline		m^{-1}
c_f	fattening parameter		$-$
c_s	skewing parameter		$-$
d	local depth		m
d'	function defined in equation AIII-13		$-$
D	particle diameter		m
E_i	internal energy		J
F_D	particle Froude number		$-$
g	gravitational acceleration on earth	9.81	ms^{-2}
g'	function defined in AIII-10		$-$
h	Chebyshev coefficients, subscript denotes order		$-$
H	Chebyshev polynomials, subscript denotes order		$-$
L	meandering channel's length		m
m	velocity profile exponent		$-$
n	transverse length		m
r	radius of curvature		m
r_c	radius of curvature at the centerline		m
s	longitudinal length		m
S_c	channel slope		$-$
S	entropy		JK^{-1}
S_T	transverse bedslope		$-$
S_{Tc}	transverse bedslope at the channel's centerline		$-$
T	absolute temperature		K
$\mathbf{v}$	velocity vector		ms^{-1}
v_s	longitudinal velocity		ms^{-1}
v_n	transverse velocity		ms^{-1}
v_{ns}	transverse velocity at the surface		ms^{-1}
Q	discharge		m^3s^{-1}
w	channel's width		m

w_e	effective width of the channel, no bankflow		m
x	length in X-direction		m
y	length in Y-direction		m
z	length in Z-direction (vertical)		m
α	ratio of projected surface area to volume for a sediment particle divided by that for sphere of the same volume		$-$
β	angle of the channel's cross direction n with valley axis		rad
ϵ	kinematic eddy viscosity		m^2s^{-1}
ζ	scaling factor used in Euler-Lagrange explanation		$-$
θ	deviation angle of channel with valley axis		rad
θ_0	deviation angle at inflection point		rad
θ'	Shield's parameter		$-$
κ	von Karman's constant	0.4	$-$
λ	meander wavelength		m
ρ	fluid density		kgm^{-3}
ρ_s	density of solid		kgm^{-3}
σ	entropy production		$Jm^{-3}K^{-1}s^{-1}$
σ_{tot}	total entropy production of one meander period		$JK^{-1}s^{-1}$
σ_{cs}	entropy production in a cross section		$Jm^{-1}K^{-1}s^{-1}$
τ	stress tensor		Nm^{-2}
ϕ	phase along the channel	$2\pi s/L$	rad
ω	specific streampower		Wm^{-2}
$_c$	subscript to denote variable at the centerline		
$_0$	subscript to denote variable at the centerline		
$_n$	subscript that gives order of Chebyshev polynomial: $0, 1, \ldots, 12$		
$\tilde{}$	superscript to denote dimensionless variable		
$\bar{}$	superscript to denote variable averaged over the depth		

Contents

Chapter 1

Introduction

All over the world natural lowland rivers and streams are winding through the sediments deposited in earlier times. Straight alluvial channels longer than about 10 to 12 times their width are rare [Odgaard, 1986a], irrespective of scale or boundary material. This winding is called meandering after the river Büyükmenderes in Turkey. This widely seen natural phenomenon has intrigued many researchers. Many theories and models are proposed to explain the process of meandering, but still meandering is not completely understood, due to the complexity of the processes involved. The most important determining quantities are the discharge and the valley slope, but also soil characteristics, vegetation cover, sediment load in the channel and the climate in the catchment area influence the process.

Despite the complexity of the meandering processes a natural meandering channel often evolves towards an equilibrium planform shape [Hooke, 2003]. Most bends in rivers and streams have not reached this equilibrium yet or will never reach it, partly because of changing conditions with time. But rivers and streams with constant properties, like constant valley slope and homogeneous bed material, develop a number of bends with similar equilibrium planform shape. This process shows self-similarity of meander geometry over a wide range of scales and environmental conditions [Knighton, 1998]. For example top-views of the Amazone river in Brazil and the Geul brook in the Netherlands cannot be distinguished on their planform shape, while one bend of the Amazone river is 250 times larger than one bend of the Geul brook. This geometric similarity makes the derivation of the meander planform shape useful. For a given ratio of channel length to valley length, it is likely that a natural alluvial meandering channel evolves towards the most probable planform shape, which is the dynamic equilibrium planform shape of meandering rivers, brooks and streams. This ratio is termed sinuosity and is equivalent to the ratio of valley slope to channel slope. It is a measure for the wiggliness of a channel.

For all these different sinuosities the meander planform shape is asymmetric [Carson and Lapointe, 1983]. This asymmetry can be demonstrated with one period of the Mississippi river's planform, see figure 1.1. This bend clearly shows that its maximum and minimum are not in the middle of the bend, but a little shifted upstream.

In our civilized world the natural bending planform shape of a meandering channel is often not desirable from economic point of view. A straight channel

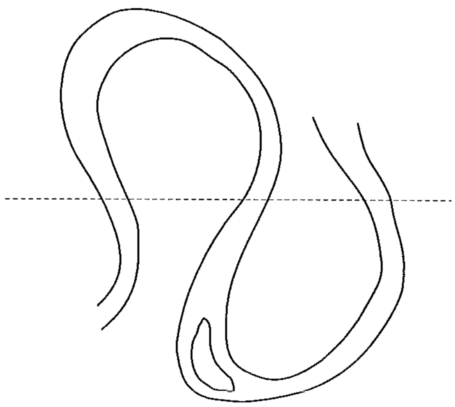

Figure 1.1: One period of the Mississippi river at Greenville, USA before artificial cut-offs with the maximum and minimum shifted upstream. The flow is from left to right and the meander wavelength is 8 km. Modified after Teuling [2002]

is more efficient for shipping transport. Moreover meandering channels change their paths in downstream direction. A channel should be stationary for many purposes, for example the land alongside the channel can be used for living or economic activities. For these reasons man has exerted considerable influence on rivers and streams and only in more remote areas large natural meandering rivers can be found. Another more indirect affect is the man induced change of land use in the catchment area. It often increases the peak discharge, because less water is stored than in the natural situation. These interferences by man are likely to affect the planform shape of a meandering channel seriously.

The aim of this research is to predict a meandering channels equilibrium planform shape for a given sinuosity. The research is mainly fundamental, but one could think of practical use in meander restoration programmes. Many channels in Western Europe are straightened in the seventies and eighties for economic reasons. A current tendency is to return to natural meandering channels, because naturally flowing brooks and rivers are considered to be more important than they were in earlier times. The meandering planform shapes are remade like they were before the straightening. Nowadays the planform shape of these newly created meanders is read from old topographical maps or soil maps. An easy alternative to find the meander planform shape from maps is the derivation of the equilibrium meander planform shape from the sinuosity.

This report is focussed on the derivation of the meandering channel's planform shape, but also the factors that determine the sinuosity are highlighted. After this *introduction* the important processes of meandering are summarized in the chapter *concepts in meandering.* All the basic concepts and theories are stated to introduce the reader into the world of meandering. The following chapters deal with the *theory* and the *model description.* The flow model and the minimization technique are explained. The *results* from the model are presented afterward. Then conclusions will be drawn and the results will be critically viewed in the *discussion.* In the last chapter, *recommendations* for future research are presented.

Chapter 2

Concepts in meandering

2.1 Introduction

Meanders are not only found in rivers and streams. In both large and small scale fluid flow the meandering pattern can be seen. Most meanders can be found in water flows. For example on glaciated inclined areas water flows can appear from melting. The resulting supraglacial channels incised in the ice may evolve to nicely shaped meanders. An example of meanders in large scale flow is the Gulfstream in the Atlantic ocean. Meanders can be seen best a little of the coast of North-America with an amplitude of several hundreds of kilometers. Also in the laboratory meanders can be created. Maybe the simplest to create are surface tension meanders. On an inclined plate with a small water stream going down, the initially straight flow evolves to a curved flow. After some time, the flow is stabilized and a meandering pattern has developed under certain plate inclinations and discharges [Culkin and Davis, 1984].

The meandering pattern is not restricted to water flow. It also exists in large scale flows of air. The large scale upper jet stream separates the cold polar air from the warm tropical air and describes a meandering pattern [Heidorn, 2002]. Much slower velocities are in the magma below the continental and oceanic crusts. Meanders are observed in these fluid flows as well.

Meanders are widely seen in fluid flows on earth. But meandering channels are not restricted to our own planet. Even on the Moon, planet Venus and planet Mars, indications of meanders are found [Komatsu and Baker, 1996]. They are probably formed by lava flows or in some cases they are likely to be formed by water flows in former wetter times.

The flow processes and sediment transport involved with the forming and shaping of meanders are complex and not completely understood. Despite this complexity, the initiation of meandering can be understood easily for an open channel with sediment in the bed: consider water flowing in a straight channel; if a very small obstacle at one side of the channel is present (for example a gravel stone), the flow velocity increases a little at the other side of the channel; this little extra power of the flow will erode more sediment from the latter side of the channel; because of the centrifugal effect the flow velocity at this side increases more, which induces again more erosion; the channel forms a bend and the erosion at the outer bend does not stop before the power of the flow is insufficient to erode more material from the outer bend. This implies that a straight channel is not stable when the flow velocity is not too small. When the flow velocity is too large, the channel will be braiding in stead of meandering [Hooke, 2003].

Braiding channels form at high sediment loads, steep valley slopes and high discharges. At high discharge, they transport and deposit sediments at high rates. The deposited sediments block their own gully and the current finds another path with less resistance. Braiding rivers often have a variable discharge, leaving the bed dry most of the year. Braiding channels are found in the erosional zone of the river, where the slope is high. Meandering rivers on the other hand are less dynamic and flow in more moderate sloping areas. The two types of rivers can be discriminated based on the sinuosity, the valley slope and the discharge. Usually a channel with a sinuosity higher than 1.5 is considered to be meandering. Braiding channels have a higher sediment load, higher peaks in discharge and the variability of the discharge during the season is normally higher. These are common criteria to differentiate between a meandering or braiding channel, but a transition zone between the two is present. A river can have a meandering pattern with braided channels in the bed or a braiding river can have some meandering pattern. Moreover the type of river that can be found in the field is not only a consequence from the conditions which can be found nowadays, also the geologic history plays a role. For instance in an uplifting area a meandering river incises in the rock and continues to meander, where for this sloping angle a braiding river would be expected. The geologic history of the river must be taken into account to understand the type of river that can be seen in the field.

To complete the different types of channels also straight and anastomosing channels should be mentioned. Straight flows in nature only occur at low slopes with a relatively low discharge. A straight channel cannot transport much sediment, because then it will change into a braiding channel. Anastomosing channels occur at very low slopes and are the stable form of a braiding channel. The discharge is too low to erode much of the bed and as a result vegetation cover exists on the islands in an anastomosing river. They can be found in lower regions of the sedimentation zone of a river. Of course intermediate forms of these types of rivers do exist as well. For example a braiding river can have some islands, that are stable for a longer period, which is a criterion for the anastomosing river. Another intermediate type of channel is a slightly curving channel. It can not yet be called meandering, but it is not straight either.

In this report the bending and shaping of alluvial meandering channels will be discussed. These are streams or rivers, that have formed their channel in the sediment that is being transported or has been transported by the channel [Schumm, 1994]. Other meanders mentioned above have different forces working, but the principle of minimal entropy production, explained later in this report, can be used on these meanders as well. In the next section the *geometric similarity of meandering channels* is discussed. Then the *interaction of flow and planform shape* is explained. Further the factors that determine the *sinuosity of meandering channels* are stated and the last section focusses on the *planform shape of meandering channels*, also the focus in this report.

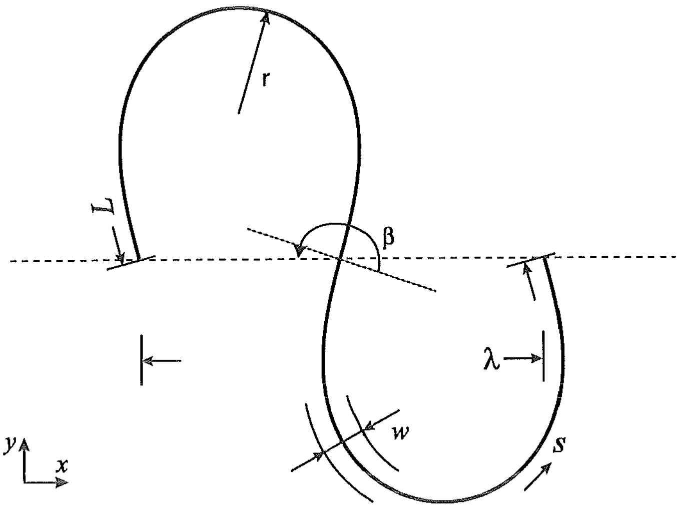

Figure 2.1: Definition of radius of curvature, wavelength, channels length and width. For the point where the channel crosses the valley axis, the angle β is defined.

2.2 Geometric similarity of meandering channels

Above it was already mentioned that meanders show geometric similarity. The wavelength (λ) and the radius of curvature (r) of a meandering channel are proportional to the channels width (w). The wavelength of a meandering channel is the traversed length in the valley direction (λ), where L denotes the channels length in this report. The radius of curvature is the radius of an imaginary circle describing the meandering channel (see figure 2.1). In a meander bend the radius of curvature is minimal (or maximal for a negative radius of curvature) at some point and then increases (decreases for a negative radius of curvature) until the inflection point. At this point the radius of curvature is $(-)\infty$, the channel is straight and the radius of curvature changes its sign. The radius of curvature thus is in the range from $-\infty$ to ∞ in one period of a meander planform. For reasons of convenience, the curvature (c) is introduced as 1 over the radius of curvature, which now has a range around zero. In figure 2.2 the meander length is related to channel width and mean radius of curvature. The plot consists mostly of meanders in rivers and in flumes, but also Gulfstream meanders and a meander on glacier ice are drawn in. From the figure of Leopold [1994] the almost linear relationship can be read:

$$\lambda = 10.9 w^{1.01} feet \tag{2.1}$$

This relation is widely used and confirmed with other situations [Davy and Davies, 1979, Hey, 1976].

Additionally, Leopold et al. [1964] found from a sample of 50 rivers differing in size as well as in geological and climatic circumstances that the ratio of radius of curvature to the channel's width has a median value of 2.7. The minimum value for this ratio in general is found to be 2.40 [Hey, 1976]. This value was

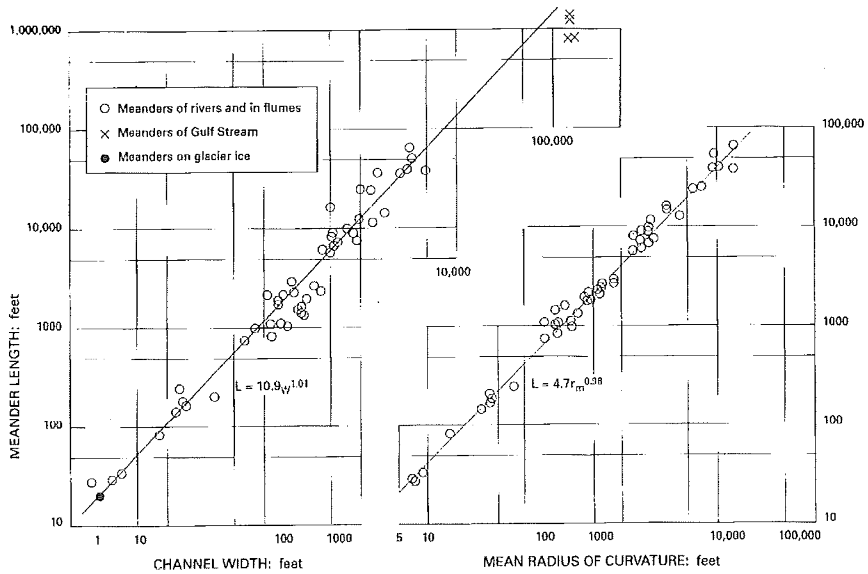

Figure 2.2: Geometric similarity in meandering channels, from Leopold et al. [1964], their figure 4.2

already compared to flow in pipes by Bagnold [1960]. In pipes the minimal energy loss or the least flow resistance in a bend occurs for a pipe with the ratio radius of curvature to the pipe diameter between 2 and 3 [Bagnold, 1960]. This range is confirmed for meandering channels by Hooke [1975]. He argued that a stable meander geometry, resulting from uniform downvalley migration, requires a radius of curvature in this range. If the ratio is smaller than 2, the resistance of the flow in both pipe and open channel will increase largely [Begin, 1981] and the flow will set free from the inner bank. This results in a widening of the bend. At higher ratios the migration rate in the upstream limb of a meander will be higher than in the downstream limb [Knighton, 1998]. Consequently the radius of curvature increases.

The ratio of radius of curvature to the channel's width in the range between 2 and 3 corresponds to the minimal ratio found in meandering planforms. This is a first indication for the tendency of a meandering channel to evolve to a planform shape, where the energy expenditure is minimal. The adjustments of the river, which may include channel geometry, slope, roughness and other variables, reflect in part changes in the rivers resistance and thus in energy expenditure [Chang, 1984]. The lower the energy expenditure, the more likely is the channel's planform shape. This is the tendency to evolve to a minimum channel slope for the given conditions [Chang, 1984].

2.3 Interaction of flow and planform shape

The meandering pattern influences the flow pattern in the channel and the flow pattern shapes the meandering pattern. This interacting system of flow and sediment in a meander bend, shows characteristic flow features that can be seen in general. The first is the superelevation at the outer bank due to the centrifugal force, that forces the water against the outer bank. The second flow characteristic is a transverse current directed towards the outer bank at the surface and directed towards the inner bank near the bed. This is the secondary circulation, that also arises from the centrifugal force.

Einstein was the first to explain this helical flow observed in rivers relating it to the flow in a flat bottomed cup with rotating tea and some tea leaves in it [Bowker, 1988]. In the outer bend in the river or near the side of the cup the centrifugal force is stronger than in the inner bend or in the middle of the cup, because the flow velocity is higher. At the bottom the flow velocity is lowest, because friction with the bed is strong. On the contrary close to the surface the flow velocity is highest. The water near the surface is forced outward more than the water near the bottom and this gives rise to fluid flow towards the outer bank near the surface. Consequently the pressure rises in the outer bend and the pressure gradient force results in a flow back to the inner bank near the bottom, because the resistance from the centrifugal force is lowest near the bed. This flow transports sediments eroded at the outer bank towards the inner bank, where point bars are comprised. In Einsteins experiment with the tea leaves in a rotating fluid, the tea leaves are homologous to the sediment in the channel and will be centered in the cup. On the contrary, another process tends to erode the inner bank. This is the Bernoulli shear process caused by an increase in flow velocity and thus more erosion in the inner bend as the pressure is lowest here [Edwards and Smith, 2002]. But this process is usually overwhelmed by the helical motion.

Einstein further noted that because the helical flow possesses inertia, the circulation (and erosion) will be at their maximum beyond the inflection point [Bowker, 1988]. Hence, the meander pattern will migrate in a downvalley direction. This is a widely accepted property of a meandering channel. Einstein also explained why larger rivers have meander patterns with longer wavelengths (see equation 2.1). Larger rivers have larger cross-sectional area, which means that helical flow will be absorbed by friction slower.

The last feature of the flow pattern in a meandering channel is a combination of the secondary circulation and the flow in downstream direction. The maximum velocity current moves from near the inner bank at the bend entrance to near the outer bank at the bend exit, crossing the channel through the zone of greatest curvature [Knighton, 1998, p. 217]. The generalized flow distribution resulting from the features discussed above is illustrated in figure 2.3.

These flow processes inherent to meandering can have different effect on the meandering system. When a meandering system has high rates of activity or migration, a high sinuosity or curvature is likely to occur. On the other hand, a meandering system can be stable with a lower sinuosity and less migration of the channel. Empirical evidence indicates that a non-linear relationship of this rate and form exists [Hooke, 2003]. To make a distinction between the stable and active meanders, we first have to consider the timescale in which a meandering channel is considered to be stable or in equilibrium. The times in geomorphology are distinguished in cyclic (10^4 years), graded (10^2 years) and steady (10^0 year) after Schumm and Lichty [1965]. Considering meandering channels, an equilibrium channel form may be expected to develop in the graded timescale. For meandering streams and brooks this time is shorter than for meandering rivers. With this division in timescale a stable meandering channel

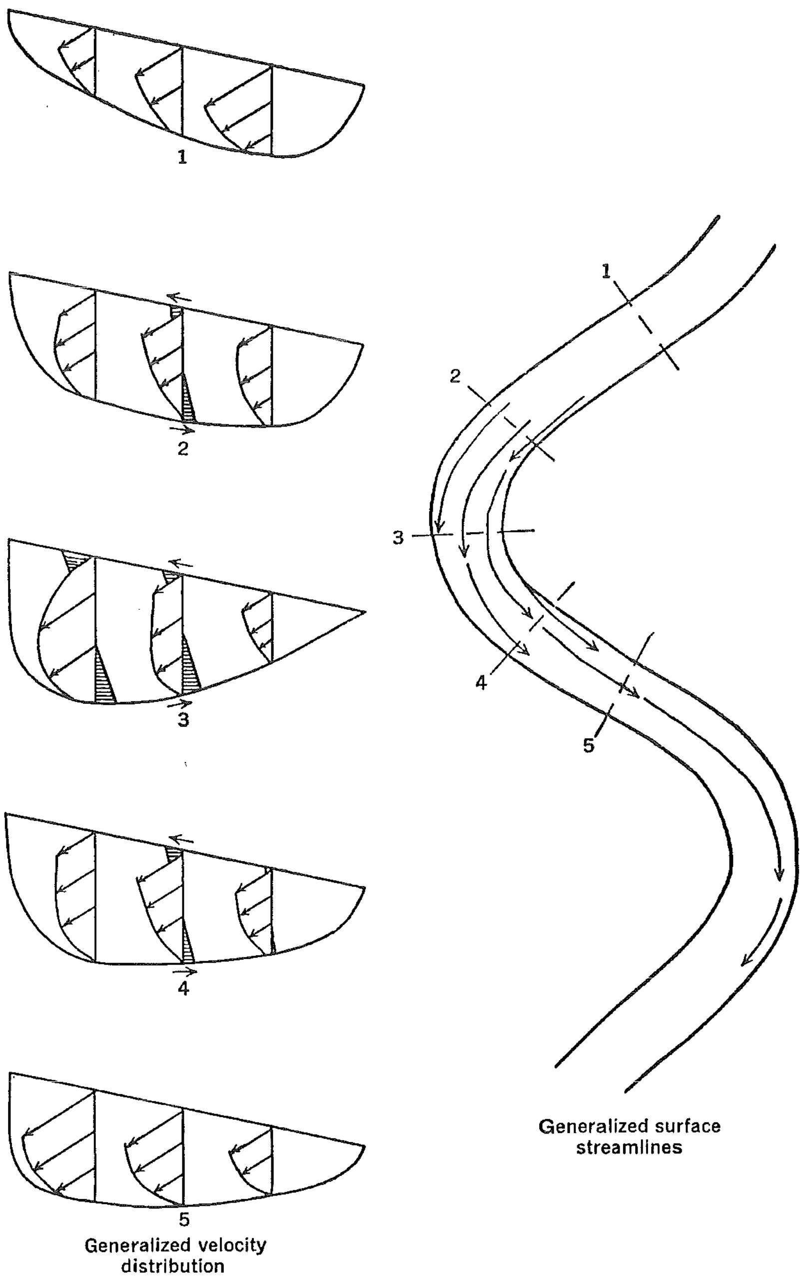

Figure 2.3: Generalized flow distribution in a meander from Leopold et al. [1964] (their figure 7-42)

can be considered to be a channel where the form is adjusted to the average upstream channel characteristics from the cyclic time (for example geology and climate). Many rivers and streams however are not stable or in equilibrium state. The migration rates and the flow are constantly changing as a result of geological uplift or subsidence, climate changes or inhomogeneities in the bed material. It is believed that these active and more stable meanders on the other hand can be found in one channel, if sufficient time is taken [Howard and Knutson, 1984, Stølum, 1996, 1998]. After a period of relative stability some cut-offs may occur and a period of rapid changes and high migration rates is present. Stølum [1996] proposed this process, with oscillations in space and time between a state in which the river planform is ordered and one in which it is chaotic, to be the self-organization process. Stølum [1996] states: "Clusters of river cut-offs tend to cause a transition between these two states and to force the system into stationary fluctuations around the critical state." In the subcritical state, the sinuosity is lower and the system is more ordered than in the supercritical, chaotic state. If cut-offs occur, order can be destroyed and the system may evolve into the more chaotic state. In the chaotic, supercritical state cut-offs are likely to bring the system over to the ordered state [Stølum, 1996]. These opposing processes self-organize the sinuosity into a steady state around a mean value for the sinuosity of 3.14 in unconstrained meanders, or the sinuosity of a circle π [Stølum, 1996]. Howard and Knutson [1984] already stated that a stabilized meander fluctuates around a sinuosity of 3.4.

The principle of self-organization is confirmed by Hooke [2003] and Hooke [2004], where the principle is illustrated with the river Bollin in England. Figure 2.4 shows the types of channels discussed above. Only the anastomosing type of channel is not in the figure, because its existence also depends on vegetation growth and it can be considered to be a special form of a braiding channel. In the meandering type of channels a division is made between active and stable meanders. In figure 2.4 the braided channels have a high bend radius of curvature and thus a low sinuosity, but a high rate of lateral movement. The active meanders have a large rate of movement, where the stable meanders have not. The active bends migrate both downstream and lateral, which results in an oblique net migration away from the valley direction. As the active meanders grow, the flow and thus the sediment transport is retarded, because of a decrease in slope and increase in form roughness. The sediment is stored in growing meanders and with a cut-off rapidly removed to the next reach [Schumm, 1994]. From the straight channels both active and stable meanders can be formed. Above the thick line the channel will evolve towards an active meander or braided channel. The dotted line is a possible plot of bend behavior. When the sinuosity gets high, the channel will form cut-offs and leave an oxbow lake. This can be either neck cut-offs when the channel cuts his own meander bend by eroding the shores, or chute cut-offs, resulting from a period with high discharges in which a preferential flow over the river sides was present (see figure 2.5). This process continues until a cluster of cut-offs results in the more ordered, stable meanders. Below the thick line (see figure 2.4), a straight channel normally evolves towards a stable meandering channel.

These stable meanders are the subject of this research. These stable meandering channels can be subdivided into low-active meanders and real stabilized meanders that have evolved to one sinuosity and rate of movement. Both forms of stable meanders can form out of a straight channel. The low-active meanders

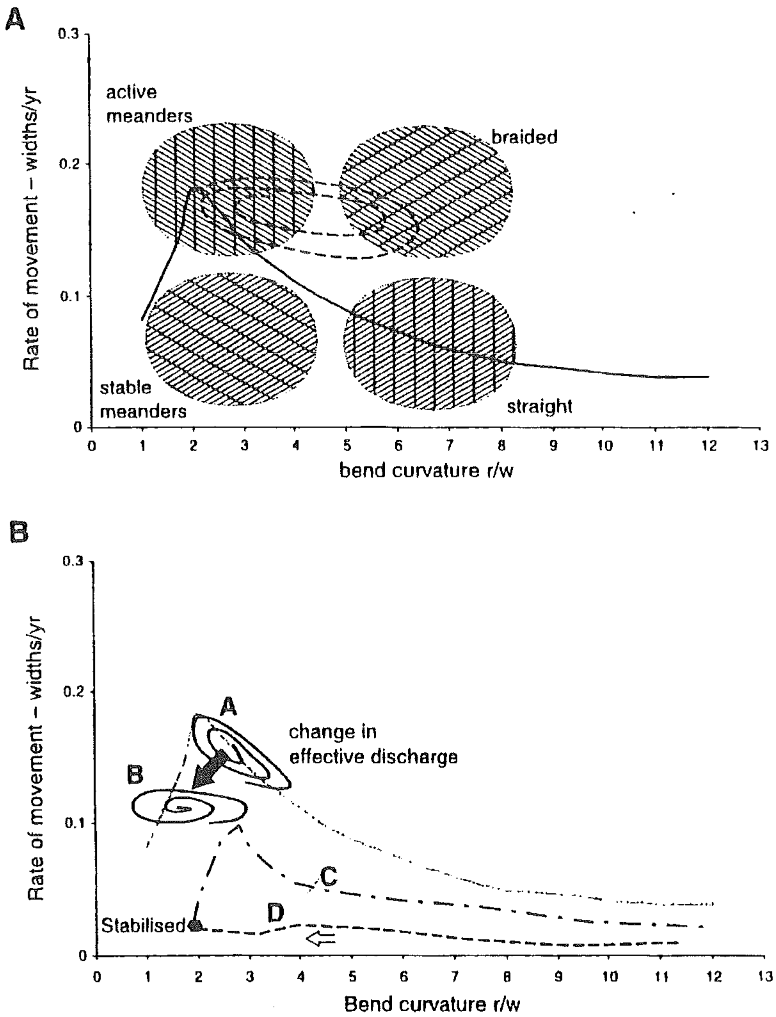

Figure 2.4: **A** Zones of different types of pattern behavior and trajectory of meandering/braiding oscillation. **B** Examples of change in meander behavior; A-B change in effective discharge; C,D alternative pathways of development of sinuous but now stable meanders. From Hooke [2003], her figure 10.

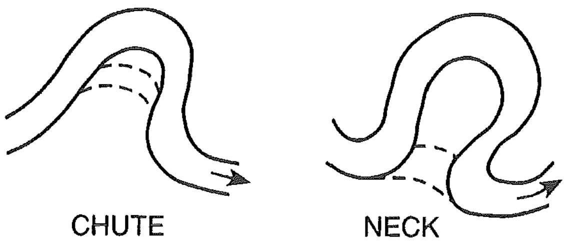

Figure 2.5: Neck and chute cut-offs

will migrate downstream, varying only slightly in sinuosity and rate of migration. Only when the conditions change dramatically they could evolve to the active meanders or braided channels. Normally they will make small movements in the shaded area of the stable meanders, where the real stabilized meanders have evolved to a stable point (see figure 2.4). Stable meanders have been reported in many papers and articles, amongst others Shams et al. [2002], Hooke [2003], Stølum [1996], Knighton [1998].

The stable meanders occurring in the cycle of self-organizing process are widely accepted. When describing this process in more detail, the equilibrium cross-section and the channels bending pattern and flow pattern are derived. Two different approaches can be followed. The first approach derives the process from deterministic calculations: the continuity and the momentum equation of both water and sediment are the constraints and the driving forces of the system. Ikeda et al. [1981] were first to state that besides the instability of the alternate-bar, which is described above as the initiation of meandering, the bend instability should be taken into account as well to describe the channel morphology. The non-linear bend equation, based on a dynamical description of flow in bends and kinematical description of bank erosion, describes the channel migration [Parker et al., 1982]. In the case of alluvial meandering channels, the two mechanisms operate at similar wavelengths, which provides a rationale for the continuous evolution of alternate bars into true bends such that each bend contains one alternate bar [Ikeda et al., 1981]. A unified bar-bend theory was developed in which a resonance mechanism operates [Johannesson and Parker, 1989, Parker and Andrews, 1986] to describe the process of meandering. This has resulted in complex three-dimensional, deterministic models, that describe the process of meandering. Assumptions made in this approach are mainly about the bottom shear stress and the description of the turbulent flow.

An alternative to these deterministic, complex models, is a variational approach using thermodynamics. Jefferson [1902] already argued that meandering is the result of a minimization of energy. Yang and Song [1979] derived the principle of minimization of energy dissipation, which is entropy production times temperature, from the continuity equation and the equation of motion. In 1945 Prigogine discovered that not only closed thermodynamical systems, but also open linear thermodynamic systems close to equilibrium evolve toward a state characterized by the minimum entropy production compatible with the constraints imposed on the system [Prigogine and Stengers, 1985]. For closed

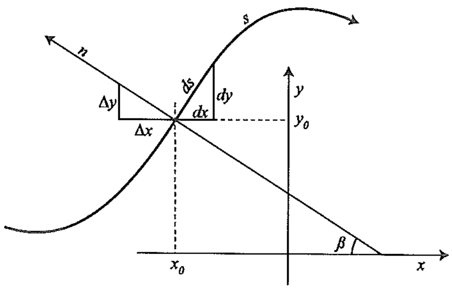

Figure 2.6: The definition of curvilinear coordinates, redrawn after Smith and McLean [1984]

systems the constraints upon the system have no effect on the final state, so the system converges to an equilibrium state where the entropy production is zero. In section 3.2 this statement is extended to be valid in non-linear open systems also. These extremal hypotheses (for example the strive towards minimization of entropy production, maximal entropy, minimum variance or minimum energy dissipation) have been criticized, because they do not consider adjustment mechanics directly and because they can give rise to unrealistic implications [Knighton, 1998]. Despite the critics on the variational approach, it is believed that both theories will lead to an explanation of the meander planform shape. With the theory based on the minimization of entropy production, the solution for the planform shape of meandering channels probably reveals less complex problems and is solved easier.

For the description of the meandering pattern resulting from the interaction between flow and sediment, curvilinear coordinates are best. The first coordinate (s) is the longitudinal length of the meandering channel, the second (n) the transverse length and the third (z) the vertical height taken from the water level. With these coordinates flow in bending systems can be described efficiently. Figure 2.6 denotes the definition sketch of curvilinear coordinates. The angle β in figures 2.1 and 2.6 is the same. Curvilinear and Cartesian coordinates are related in appendix II taken from Teuling [2002].

2.4 Sinuosity of meandering channels

The sinuosity of a meandering channel was already defined to be the ratio of channel length over valley length or valley slope over channel slope. To predict an alluvial meandering channel's sinuosity quantitatively from different channel characteristics is difficult, if not impossible [pers. comm. E. Mosselman]. The variables are interrelated and have different impacts in different channels. The number of variables is higher than the number of equations that can be used. Width, depth, velocity profile, slope, sediment load in the water, sediment load in the bed, hydraulic roughness, vegetation growth and (variability in) discharge all influence the sinuosity, which the channel evolves to. The most important feedbacks limiting the extent of meander development are the reduction in energy gradient and the rise in resistance to flow with higher sinuosity [Ferguson, 1973, Knighton, 1998]. In this section the most important qualitative and some quantitative characteristics are summarized.

First of all the slope of the valley is the most important factor determining the sinuosity of a meandering channel. Together with the amount of water available, the discharge and thus flow velocity is governed by valley slope. If the slope is high and the channel is not yet braiding, the sinuosity is high. Schumm et al. [1972] related the valley slope to the sinuosity in an experimental study with different sediment loads and similar discharges in channels and bends in the Mississippi river. With increasing slope starting with a horizontal valley, he found a straight channel gradually changing into a meandering channel and the sinuosity increasing gradually also. At some higher slope Schumm et al. [1972] found the meandering channel to change sharply into a braiding channel with a sinuosity slightly higher than 1. This could be done for this particular river, but differences between channels in the amount of water available for run-off have to be taken into account. A nice example that illustrates this, is the river Rhine. When during the last ice age, the discharge was considerable higher because of meltwater, the river was braiding in stead of showing the current meandering pattern.

Together with slope, the discharge of the river is important. The discharge varies during the year, but the discharge at bankfull stage occurring once or twice a year on average governs both sinuosity and planform shape. This is widely accepted. It can be explained from the fact that higher floods do not occur often and induce cut-offs in stead of a stable channel. Lower discharges do not have the erosion power, which is available at bankfull stage. The slope and discharge are combined in one variable, the streampower. The specific streampower (ω) is the streampower divided by the width of the channel. In formula form this is:

$$\omega = \frac{\rho g Q S_c}{w} \tag{2.2}$$

The more energy is present, the higher the specific streampower and the higher the sinuosity of a meandering channel. This also implies that the specific streampower can be used to make a distinction in meandering and braiding type of channel. Nanson and Croke [1992] proposed that a specific streampower below $50 - 60\,W/m^2$ will form meandering channels and higher numbers are in accordance with braiding channels.

Another channel characteristic that is not included in the specific streampower and certainly influences sinuosity, is sediment load. The load carried by natural streams and rivers can be separated in dissolved load, wash load and bed-material load. The dissolved load consists of the material transported in suspension. The wash load is transported and temporarily maintained in the flow by turbulent mixing processes and the bed load are those particles that move by rolling, sliding or saltation [Knighton, 1998]. When a channel transports a mix of these loads, the bank stability is higher than channels with only bed load. Channels with a mixed load result in a narrower and deeper channel with a possibly higher sinuosity than channels that mainly transport sediment smaller than medium sand [Shams et al., 2002, Knighton, 1998]. This is confirmed by Schumm et al. [1972], Ferguson [1975], who state that the sinuosity increases with the silt-clay content of the banks. But bank-material composition is highly variable at different channel sites and differences in cohesiveness and erodibility between layers makes a quantification difficult. Information on the relationship between sediment load and meander form is meagre [Knighton, 1998].

Also the relationship of form and vegetation growth is not very clear and hard to quantify. Vegetation holds the bank material and increases the hydraulic roughness of the channel. Just as for the mixed sediment load, channels with denser vegetation give rise to a narrower and deeper channel [Knighton, 1998]. Also a seasonal effect can be seen in some channels. From a practical study at the Keersop stream by Wolfert [2001] it follows that plant growth in summer divides the stream. Between the vegetation beds chutes do occur and the helical cells are disrupted. In winter the stream is clean and higher peak discharges are present. The chute channels are filled and erosion of the inner bank prevails. This seasonal effect influences the bedform configuration and the sinuosity [Wolfert, 2001].

2.5 Planform shape of meandering channels

Langbein and Leopold [1966] found that the meandering path reflects somehow a state of maximum likelihood. They proposed a sine-generated curve, which has the property to minimize the sum of the squares of the changes in direction (changes in width, depth, velocity, shear and Darcy-Weisbach friction). This was the basis for the theory of minimum variance, stating that meanders are characterized by a minimum variance not only of angular deflection, but also in hydraulic properties [Teuling, 2002]. This theory can be interpreted as a strive to uniformity in the rate of energy expenditure [Leopold and Langbein, 1966]. It proved to be an oversimplification of the meander planform, because the theory did not account for bed topology (the pool-bar sequence) and helical motion [Teuling, 2002]. Also Carson and Lapointe [1983] concluded that the theory of minimum variance should be discarded. From inspection of 15 rivers' data they found statistical evidence for 2 asymmetries in meandering rivers. The first is a downchannel delay in the inflection point of meanders. This means that the curvature is changing sign after the channel has past the center of the valley. The second asymmetry is an upvalley skew or displacement of the minimum and maximum of a meandering bend [Carson and Lapointe, 1983]. These asymmetries appeared not to depend on whether the meander was migrating freely, was constrained laterally or was incised in rock. For an explanation of these asymmetries, the persistence of helical circulation and cross-section distribution of the longitudinal velocity is of major importance [Carson and Lapointe, 1983]. The flow pattern adjusts well past the bend that forms them. This is in accordance with downvalley migration of the bend as explained above. Another characteristic feature of the shape of the meander planform is that bends are full and rounded or fattened in respect with a first order sine-generated curve [Parker et al., 1982].

Parker et al. [1982] explained the fattening and skewing of meandering channels with a non-linear stability analysis. This was based on the equation of bend migration [Ikeda et al., 1981]. Figure 2.7 illustrates that a meandering reach intensifies fattening and skewing as lateral and downstream migration progress [Parker et al., 1982]. This combined dynamic description of flow in bends and the kinematic description of bank erosion, resulted in the formulation of a third order sine-generated curve or the Kinoshita curve to describe meander bends:

$$\theta(s) = \theta_0 \, cos\phi - \theta_0^3 \left(c_f \, cos3\phi + c_s \, sin3\phi\right) \tag{2.3}$$

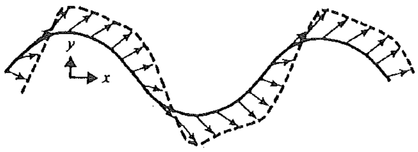

Figure 2.7: The formation of fattening and skewing in meandering channels, from Parker et al. [1982]

Here, θ is the angle of channel with valley axis, θ_0 is this angle at the first inflection point and c_f and c_s are the fattening and skewing parameters, respectively. For high-amplitude meander bends Parker et al. [1983] found a prominent skewing with the bend instability analysis. The equilibrium with skewing is unstable at lower amplitude, for higher amplitude bends the stability is unknown [Parker et al., 1983]. This reflects that with the deterministic approach, the fattening and skewing of meandering channels is not perfectly understood.

Chapter 3

Theory

3.1 Introduction

With the basic concepts in meandering summarized, focus is now laid on the planform shape of a meandering channel. This research starts from Andel [2002] and Teuling [2002]. They have already derived the most probable periodical planform shape of a meandering channel from entropy concepts. Their results show similarities with stable meandering channels found in nature, but they used two unsatisfactory steps in the reasoning procedure. The first assumption is that a meandering channel evolves to a planform shape that can be generated from a third order sine-curve (see equation 2.3). This assumption was based on the article of Parker et al. [1982]. In this article the meandering channel's planform shape is the result of deterministic calculations. This result does not guarantee that the most probable planform shape derived from entropy concepts is a third order sine-generated curve. Moreover a delayed inflection point cannot result from this curve. For these reasons the planform shape in this research is derived without any assumptions regarding the planform shape of a meandering channel, but the assumption of periodicity of the meander planform. From a given sinuosity, the equilibrium planform shape of a stable meandering channel is derived by minimization of the entropy production. The second unsatisfactory step in the reasoning procedure is about the entropy concept. Andel [2002] and Teuling [2002] based their research about the entropy concept on the assumption that the state to which a meandering river evolves is one in which the variance in entropy production is minimal [Teuling, 2002]. This chapter shows that it is not the entropy production variance that has to be minimized, but the total entropy production over one period of a meandering channel.

In the next section of this theory chapter the reasoning to end up with this latter entropy statement is presented. After founding evidence for this general statement is provided, the statement is applied to meandering channels in section *entropy production minimization in meandering channels.* In this section the total entropy production equation for meandering channels is derived and explained. In the last section the *minimization technique* used to minimize the total entropy production is explained. The problem of finding the most probable planform shape can be well cast as an optimal control problem, for which minimization can be done with variational procedures.

3.2 Entropy production minimization in open systems

Entropy of a system is a quantity that denotes the state of chaos in the system. For fluid flow in open channels, like meandering rivers and streams, more turbulence generally means higher entropy. In 1854 Clausius introduced the term as a measure of the dissipated potential. Many different definitions of entropy have been proposed in terms of probability or statistical variables. In this research only the thermodynamic entropy is used and thus only this definition is stated. In thermodynamics, the change in entropy (S) between two states A and B is defined as the integral of the ratio of change in internal energy (E_i) to absolute temperature (T) [Ohanian, 1989, p. 559]:

$$S_B - S_A = \int_A^B \frac{\mathrm{d}E_i}{T} \tag{3.1}$$

This expression clarifies the relation between entropy and energy. For a system with constant temperature, the entropy and energy can be interchanged in qualitative reasoning.

With this definition of entropy the second main law of thermodynamics can be stated: the entropy of a closed system must increase or remain the same. At equilibrium state the entropy is maximal for closed systems, so no entropy is produced anymore. With this second main law the direction of time is defined. Entropy cannot be transformed into work. Once mechanical work is transferred into entropy, this can not be reversed back into mechanical work. This irreversibility implies that every system develops towards a dissipation of potentials [Teuling, 2002]. The entropy at state B is larger or equal to the entropy at state A. For an open system this classical approach of entropy cannot be used. Clearly a meandering channel is an open system. The constraints upon the system and the open boundaries generate continuously entropy. An open system will not evolve to an equilibrium state, where the entropy production is zero. But Prigogine [1945] found that linear thermodynamic systems close to equilibrium evolve "toward a stationary state characterized by the minimum entropy production compatible with the constraints imposed on the system" [Prigogine and Stengers, 1985]. The entropy production per unit time and volume (σ) can only decrease in such systems for time independent boundary conditions [Glansdorff and Prigogine, 1964]. At the stationary state itself the entropy production is minimal. Then the rate of entropy outflow is equal to the rate of entropy production.

The statement of Prigogine [1945] is only valid for linear thermodynamic systems. This linearity means amongst others, linear relations between forces and rates and constancy of phenomenological coefficients like thermal conductivity and diffusion coefficients [Glansdorff and Prigogine, 1964]. This is not the case for a channel containing water flow, because the flow in most channels is turbulent. Reynolds numbers of streamflows are normally in the order 10^5, where turbulence begins to become persistent in open channels at a Reynolds number of about 500 [Davy and Davies, 1979]. Prigogine states [Davy and Davies, 1979]: laminar flow in open channels on the other hand "corresponds to a minimum of energy dissipation. Under isothermal conditions this is equivalent to minimum entropy production. Laminar flow corresponds to the state of the system near thermodynamic equilibrium." Laminar flow in open channels can be considered as a linear system. Meanders formed out of laminar flow can be found in surface tension meanders. These meanders on an inclined plate show the typical asymmetry in meander planform shape found in nature and they tend to a steady state [Teuling, 2002]. This implies that flow conditions are of little importance for applicability of the minimal entropy production concept [Teuling, 2002]. The surface tension meanders with typical planform shape are in equilibrium state while turbulent channel meanders are also in steady state with similar planform shape. Another argument for the statement of Prigogine to be valid is the mathematical derivation of the theory of minimum rate of energy dissipation by Yang and Song [1979] based on the equations of motion and continuity. The dynamic nature of channels can be described by this theory. Meandering and braiding channels are distinguished on the entropy production quantity, which forms another indication for the validity of this criterion. Meandering channels usually flow on smaller slopes and have a lower entropy production for the same discharge.

A stronger reasoning would be to extend the statement of Prigogine [1945] to open systems generally. Reiser [1996] realized that the statement of Helmholtz [1868] (statement of Helmholtz and Rayleigh) also treats the principle of minimal entropy production. Both statements of Helmholtz and Rayleigh and Prigogine are valid with their restrictions. The first holds for general and time-dependent flow processes which are only restricted by a certain connection to source fields and the latter holds for general linear processes but restricted to stationary processes [Reiser, 1996]. This is an indication for a more general principle of entropy production that covers both statements of Prigogine and Helmholtz and Rayleigh [Reiser, 1996]. The statement of Helmholtz and Rayleigh is that the entropy production is minimal under the restrictions of the Helmholtz condition. The essential point of the derivation of the statement of Helmholtz and Rayleigh, named the Helmholtz condition, is that the Laplacian of the velocity for which the continuity equation holds ($\nabla \cdot \mathbf{v} = \mathbf{0}$) has to be a source field [Reiser, 1996]. This reads:

$$\mathbf{s} = \Delta \mathbf{v} = \nabla Q \tag{3.2}$$

where Q is a scalar potential and $\mathbf{s}$ is a vector. An interpretation of equation 3.2 is a representation of vector $\mathbf{s}$ by a potential Q, a source field [Reiser, 1996]. To generalize the statement of Helmholtz and Rayleigh (1868) this representation should be a general vector field. With the Clebsch Ansatz [Clebsch, 1859] the generalization can be made and the generalized representation of the vector $\mathbf{s}$ reads:

$$\mathbf{s} = \nabla Q + h \nabla R \tag{3.3}$$

where h and R are scalar functions similar with Q [Reiser, 1996]. With the condition of Caratheodory (1930) and realizing the Clebsch condition can be treated by the method of an integration multiplicator initiated by Pfaff [1815], the same conclusion can be drawn as for the statement of Helmholtz and Rayleigh (1868) Reiser [1996]. The statement of Helmholtz and Rayleigh holds not only for velocities obeying condition 3.2, but also for general velocity fields (equation 3.3) [Reiser, 1996]. The generalized statement of Helmholtz and Rayleigh explains many different extremal principles of irreversible thermodynamics and this leads to the consideration of the principle of minimal entropy production as a fourth main law of thermodynamics [Reiser, 1998]. This law contains the evolution principle of Glansdorff and Prigogine [1964] as a special case [Reiser, 1998]. With the generalized principle of minimal entropy production, balance equations like the momentum equation can be simplified [Reiser, 2000]. Solutions may be analytical in stead of only numerically available [Reiser, 2000]. For example the Hagen-Poiseuille flow and Couette flow can be derived in an elegant way by means of the principle of minimal entropy production [Reiser, 2000]. Particularly for more complicated processes this treatment is relatively easier than derivation from the balance equations [Reiser, 2000].

With this generalization of flow fields, the principle of minimal entropy production is no longer restricted to linear thermodynamic systems close to equilibrium. The principle of minimal entropy production can be applied to non-linear open systems as well. For the meandering channel's planform this means that the shape, at which minimal total entropy production occurs, is the optimal planform shape for stable meandering channels. The equations to compute the total entropy production used to determine the optimal meander planform shape are presented in the next section. The interpretation concerning the optimal optimal shape of a meandering channel derived from this principle of minimal entropy production is that a channel reduces its velocity to minimize friction loss of the channel with the shore [Reiser, 2003].

3.3 Entropy production minimization in meandering channels

Entropy production minimization can be used for a large number of (geomorphologic) processes. For the reconstruction of dynamical systems from data, which are only partially available, methods are needed to extract the underlying dynamics: besides statistical methods, estimation of parameters and filtering, entropy production minimization is one of them. For example an optimal river basin network is generated by minimizing energy expenditure by Carcho and Sol [2002]. This minimizing energy expenditure is equivalent to entropy production minimization. This example is hydrological, but the same theory is used in biology too. The optimal structure of a branching tree, the inner lung structure or the blood vessel structure is derived from minimization of entropy production. The derived optimal structures are similar with structures found in nature. Another example where the entropy principle is used is in wave physics. The only way to distinguish between waves and their reflected waves with the same amplitude, period and (group) velocity is to use the entropy term (pers. comm. T. Hoitink, 2003).

To derive the most probable planform shape of a meandering channel the principle of minimal entropy production will be used here. By minimizing the total entropy production, the most probable planform shape of a stable meandering channel can be derived. For a given sinuosity a stable meandering channel has similar planform shape to other channels with the same sinuosity, regardless of sediment in the bed, slope, discharge, vegetation, climate or other variables that effect the channel (see section 2.2).

Another argument in favor of the use of the theory of minimization of entropy production is that the meandering pattern occurs also in flows without sediment, for example in supraglacial streams, surface tension meanders on an inclined plate or the large scale meanders in the Gulfstream in the Atlantic Ocean. This implies a more general principle than mere sediment transport. It is proposed here that entropy production minimization is this profound principle which follows from physical laws. Before minimization of the total entropy production is possible, the total entropy production for arbitrary planform shape must be computed.

In an isothermal system the entropy production is only caused by irreversible friction losses within the fluid [Davy and Davies, 1979]. A meandering channel can be considered to be isothermal, because the heat production by friction is only small. If the fluid is also considered to be incompressible, the entropy production per unit volume and unit time, σ, is described by [Yang, 1992]:

$$\sigma = -\frac{1}{T}(\tau : \nabla \mathbf{v}) \tag{3.4}$$

In this equation T is the absolute temperature, τ is the stress tensor and $\mathbf{v}$ is the velocity vector. The equation is obtained from combination of the first law of thermodynamics with the equation for an isothermal system and incompressible fluid [Teuling, 2002]. In terms of energy the derivation can be found in many handbooks on fluid mechanics, such as Bird et al. [1960]. This derivation is shown in appendix I, taken from Teuling [2002].

In a meandering channel the flow is turbulent. To be able to describe the stress tensor, the turbulent flow can be described by means of the kinematic eddy viscosity (ϵ). This is similar to kinematic viscosity in laminar flow, but the kinematic eddy viscosity is often much larger than the kinematic viscosity [Douglas et al., 1985]. If the kinematic eddy viscosity is used to approximate the average flow velocities (in longitudinal and transverse directions) of turbulent flow, this implies that the influences of turbulent flow on the meander planform are neglected [Teuling, 2002]. Odgaard [1986a] and Smith and McLean [1984] also used this assumption. This results in the following description of the stress tensor (see appendix II by Teuling [2002], equations AII-18 a and b):

$$\tau_{ij} = -\rho\epsilon(\nabla v_{ij} + \nabla v_{ji}) \tag{3.5}$$

The subscripts i, j represent pairs of the coordinate directions s, n and z. These are curvilinear coordinates, explained in the concepts in meandering chapter and appendix II. The velocity gradient tensor in curvilinear coordinates is derived from the $\nabla \mathbf{v}$ in Cartesian coordinates in appendix II. From this tensor the different stresses can be derived, but the complete determination is complex. Fortunately, several components can be neglected, because they are not important for the situation of a moderately meandering, shallow channel with steady, subcritical flow. This assumption of steady flow implies that the meander planform is determined by one unique discharge [Teuling, 2002]. The assumption of bankfull discharge being this unique discharge is widely used in meander literature, for example Parker et al. [1982], Parker et al. [1983], Ikeda et al. [1981], Chang [1984], Odgaard [1986a] and Odgaard [1986b]. This dominant discharge occurs when the channels cross section is just filled and has a recurrence interval of 1-2 years [Knighton, 1998].

For the situation described above the velocity gradient tensor can be simplified. The normal stresses disappear because the fluid is considered to be incompressible. Moderately meandering means that the ratio of width to radius of curvature is small, which makes $\frac{\partial v_s}{\partial n}$ and $\frac{\partial v_n}{\partial s}$ small compared to $\frac{\partial v_s}{\partial z}$

and $\frac{\partial v_n}{\partial z}$. Also the assumption of shallow channels (width is large compared to depth) implies this simplification, but furthermore makes the bankflow region unimportant [Andel, 2002]. The velocity gradients $\frac{\partial v_z}{\partial s}$ and $\frac{\partial v_z}{\partial n}$ can therefore be neglected. With this simplification the calculation of the tensor product (equation 3.4) results in an expression for σ only dependent on the vertical gradients of the longitudinal and transverse velocity [Andel, 2002]. This derivation is shown in more detail in appendix II, taken from Teuling [2002].

$$\sigma = \frac{\rho\epsilon}{T}\left(\left(\frac{\partial v_s}{\partial z}\right)^2 + \left(\frac{\partial v_n}{\partial z}\right)^2\right) \tag{3.6}$$

In appendix II this equation 3.6 is derived for a river. Some relations and reasoning are explained more below. A first remark is about equation AII-3 in appendix II, which relates the curvilinear equations to Cartesian coordinates. All variables in this expression have the dimension length except for the cosine and sine. This is important to realize, because it could be interpreted as a dimensionless variable. The variable s is the length along the channels centerline, beginning for example at an inflection point. The subscript 0 in this equation denotes the coordinates at the centerline. This subscript is used in equation AII-4 as well. This relation is the radius of curvature only valid at the centerline. The more general expression for the radius of curvature (r) [Harris and Stocker, 1998, p. 520] is valid in the whole channel:

$$r = \frac{\left((\frac{\mathrm{d}x}{\mathrm{d}s})^2 + (\frac{\mathrm{d}y}{\mathrm{d}s})^2\right)^{\frac{3}{2}}}{\frac{\mathrm{d}x}{\mathrm{d}s}\frac{\mathrm{d}^2y}{\mathrm{d}s^2} - \frac{\mathrm{d}^2x}{\mathrm{d}s^2}\frac{\mathrm{d}y}{\mathrm{d}s}} = \left(-\frac{\mathrm{d}\beta}{\mathrm{d}s}\right)^{-1} \tag{3.7}$$

For $n = 0$ equation AII-4 follows directly. Both equations are relations for the radius of curvature. This radius of curvature tends to infinity if the channel is straight, for example at the inflection points. For sharp parts of the bend, the radius of curvature divided by the channels width is in the order of 2-3. To circumvent this large range and to have continuous derivatives with respect to the longitudinal coordinate s, the curvature (c) is introduced. The relation with the radius of curvature is simply $c = \frac{1}{r}$. The range for this curvature divided by channel's width is (-0.5; 0.5). The negative values denote a negative radius of curvature. The curvature of a simple, one period sine is negative in the first part and positive in the range $(\pi, 2\pi)$. To relate the curvature at the centerline (c_c) and the curvature (c) anywhere else the following expressions can be used:

$$c = \frac{1}{r} = \frac{1}{r_c - n} = \frac{1}{c_c^{-1} - n} = \frac{c_c}{1 - nc_c} \tag{3.8}$$

The last expression from equation 3.8 agrees with equation 3.7. This can be seen, when the relations for x and y and their derivatives with respect to s are substituted. The result is an expression similar to equation AII-7 for the first scaling factor. The numerator of equation 3.7 then is $(1 - nc_c)^3$. The denominator of this equation has to be $c_c(1 - nc_c)^2$ to agree with equation 3.8. This can be found by replacing the derivatives of the denominator with derivatives valid only at the centerline. Then working out the bracketed terms and using equation AII-3 to relate the derivatives valid at the centerline with the angle of the cross direction n and the valley axis (β), yields an equation for the curvature with only c, c_c, n and sines and cosines from this β. The latter can be replaced by the curvature at the centerline and the denominator is indeed found to be $c_c(1 - nc_c)^2$.

Because the interest of this research is to compute the total entropy production of one channel period (σ_{tot}) relation 3.6 is integrated over the cross section and over the longitudinal centerline length of one meander period. The resulting relation is equation 3.9, in which w_e is the effective channels width, d the local depth and L the distance along the centerline of one period of the meander. The effective channel's width is introduced as the part of the channel not influenced by bankflow.

$$\sigma_{tot} = \frac{\rho}{T} \int_0^L \int_{-\frac{1}{2}w_e}^{\frac{1}{2}w_e} \int_0^d \epsilon \left(\left(\frac{\partial v_s}{\partial z} \right)^2 + \left(\frac{\partial v_n}{\partial z} \right)^2 \right) dz dn ds \tag{3.9}$$

3.4 Minimization technique

To derive the most probable planform shape of a meandering channel the principle of minimal entropy production can be used. By minimizing the total entropy production the most probable planform shape of a stable meandering channel will be derived. This comes down to optimization (in this case minimization) of the cost function, which is the total entropy production. One optimization technique is variational methods. To find the minima or maxima of a function of more than one variable, which has to satisfy certain constraints on these variables, this technique is widely used. Another name for this mathematical method is calculus of variations, of which examples are found in many research subjects [Wylie and Barrett, 1982].

Probably the easiest and most obvious example is the problem to find the shortest path between two points. Of course the solution of minimization of the integral, that corresponds to the length of the line, is a straight line.

Another more difficult example is minimization of the remainder of measured and modelled data. In this way models are improved to fit better with reality without losing the satisfaction of the constraints on the system. This is done by introducing adjoints. These extra equations help to derive the minimum. This method is named variational data-assimilation, which is often used in meteorology and physical oceanography [Cadallero, 1994] [Vos, 2002].

These are just two examples. The calculus of variations is also used in minimizing time or financial cost for complex industrial processes or to make robots or machines work in the most efficient way.

Generally the minimum or maximum of a function of more than one variable can be derived by using the Euler-Lagrange equation, if the function is to extremize an integral, which includes the variables of the function [Wylie and Barrett, 1982]. The function must satisfy this differential equation at all points and times. If the Euler-Lagrange differential equation is satisfied, this is not necessarily the solution of the problem. The Euler-Lagrange equation can be compared to the adjoints in the second example. For complex problems this relation can simplify solving the problem. This is true for the derivation of the optimal planform shape for a meandering channel. The Euler-Lagrange equation for this particular problem is derived below from the dimensionless total entropy production (see model description chapter) of one period of a meandering channel, which is indeed an integral. The derivation for this problem is based on Wylie and Barrett [1982], where a general function is minimized.

The starting point for the derivation of Euler-Lagrange equation for the problem of finding the optimal meander planform shape is equation 3.10, which results from analytic calculations on equation 3.9 in appendix IV, explained later in this report. This equation is not directly a function of the curvature, but all variables in the equation are a function of this curvature or its partial derivatives. So the integrand is a function of s, n, c, c_s and c_n. The dependence on the partial derivatives is crucial, because without these the resulting Euler-Lagrange equation does not add any information to the problem. In this section subscripts for this curvature (c) mean the partial derivatives with respect to this direction.

$$\sigma_{tot} = \kappa^2 \int_0^L \int_{-\frac{1}{2}}^{\frac{1}{2}} (a\,\bar{v}_s{}^3 + b\,\bar{v}_s\,v_{ns}^2)\,\mathrm{d}n\mathrm{d}s = \kappa^2 \int_0^L \int_{-\frac{1}{2}}^{\frac{1}{2}} f(s,n,c,c_s,c_n)\,\mathrm{d}n\mathrm{d}s \tag{3.10}$$

Now suppose that this function f is twice differentiable with respect to any combination of its arguments. Also suppose a function $c = c(s,n)$ exists, which is twice differentiable on the domain, which satisfies the end conditions of the integral and which minimizes the cost function (σ_{tot}). Under these assumptions the minimizing function for the curvature is determined. With this derivation of the Euler-Lagrange equation the constraints on the system are not included. The problem would be too complex to explain here. For an extension of the derivation with constraints, mathematical handbooks like Wylie and Barrett [1982] can be used. This extension is based on the implementation of Lagrange multipliers, which are arbitrary constants for integral constraints. For the meandering problem the constraints are not integrals. This should be circumvented by choosing suitable comparison functions. In this way the Lagrange multipliers are not constant anymore, but are a function of the longitudinal coordinate (s).

The next step towards the unconstrained Euler-Lagrange equation is to write the curvature with an additional term, where ζ denotes a scaling factor and both C (new curvature) and η (arbitrary function of s and n) are only defined in this section:

$$\begin{aligned} C(s,n,\zeta) &= c(s,n) + \zeta\,\eta(s,n) \\ C_s &= c_s + \zeta\,\eta_s \\ C_n &= c_n + \zeta\,\eta_n \end{aligned} \tag{3.12}$$

This can be done if both the introduced η and C are twice differentiable with respect to s and n and if this new curvature function has the same value at the boundaries of the integral for the new and the former curvature:

$$\begin{aligned} \eta(0,n) &= \eta(L,n) = 0 \\ \eta(s,-\frac{1}{2}) &= \eta(s,\frac{1}{2}) = 0 \\ C(0,n,\zeta) = c(0,n),\ & C(L,n,\zeta) = c(L,n) \\ C(s,-\frac{1}{2},\zeta) = c(s,-\frac{1}{2}),\ & C(s,\frac{1}{2},\zeta) = c(s,\frac{1}{2}) \end{aligned} \tag{3.14}$$

Now the entropy production is a function of the newly introduced C instead of c. If we differentiate with respect to ζ, the scaling factor in the new curvature, we end up with the following equation:

$$\begin{aligned}\frac{d\sigma_{tot}}{d\zeta} &= \kappa^2 \int_0^L \int_{-\frac{1}{2}}^{\frac{1}{2}} \left(\frac{\partial f}{\partial C}\frac{\partial C}{\partial \zeta} + \frac{\partial f}{\partial C_s}\frac{\partial C_s}{\partial \zeta} + \frac{\partial f}{\partial C_n}\frac{\partial C_n}{\partial \zeta} \right) dnds \\ &= \kappa^2 \int_0^L \int_{-\frac{1}{2}}^{\frac{1}{2}} \left(\frac{\partial f}{\partial C}\eta + \frac{\partial f}{\partial C_s}\eta_s + \frac{\partial f}{\partial C_n}\eta_n \right) dnds\end{aligned} \tag{3.15}$$

For $\zeta = 0$ the new curvature (C) is again the former curvature c. The entropy production has a minimum for an existing function c, because we know that a minimum is present in the total entropy production of a meandering river. So equation 3.15 can be set equal to 0. After partial integration of the second and third term of the integrand (where the condition for η to be 0 at the boundaries is used), the equation has the following form:

$$\frac{d\sigma_{tot}}{d\zeta} = \kappa^2 \int_0^L \int_{-\frac{1}{2}}^{\frac{1}{2}} \eta \left(\frac{\partial f}{\partial c} - \frac{\partial}{\partial s}\frac{\partial f}{\partial c_s} - \frac{\partial}{\partial n}\frac{\partial f}{\partial c_n} \right) dnds = 0 \tag{3.16}$$

To fulfill this integral with the conditions for η taken into account the integrand without η has to be 0 [Wylie and Barrett, 1982, Lemma 1, p. 827]. This is the Euler-Lagrange equation in curvilinear coordinates:

$$\frac{\partial f}{\partial c} - \frac{\partial}{\partial s}\frac{\partial f}{\partial c_s} - \frac{\partial}{\partial n}\frac{\partial f}{\partial c_n} = 0 \tag{3.17}$$

We must be careful with this Euler-Lagrange equation, because it is not a sufficient condition to minimize the corresponding cost function (the integral for total entropy production). The fact that $\zeta = 0$ is a value which makes the derivative of the cost function zero, implies only that it is a stationary point, where the cost function has a minimum or maximum or a horizontal inflection point [Wylie and Barrett, 1982]. And even if a minimum occurs, it may be a local minimum in stead of the absolute minimum.

The problem to find the optimal planform shape of a meander is complex. This makes a numerical approach inevitable. The Euler-Lagrange equation can be used to find the optimal planform shape of a meander, but the problem could not be solved alone by using this extra equation. For this reason an existing optimization technique was searched for to solve the minimization problem. It turned out that the problem can be formulated as an optimal control problem with constraints.

At Wageningen University, the systems and control group uses and develops optimal control software. Among the application areas are indoor climate control (greenhouses, stables, storage buildings), the control of mechanical systems (agricultural field machines, a tomato picking robot), processes in the food industry (sterilization, drying) and economics [http://www.aenf.wau.nl/mrs/]. A complete different application of optimal control problems is the problem of finding the optimal meander planform shape. Below the optimal control theory is explained based on Vlassenbroeck and Dooren [1988], Willigenburg [2003], Lambregts [1995] and Bryson jr. and Ho [1975].

In optimal control problems a criterion is minimized and the system equations are equality constraints [Lambregts, 1995]. For this system the state variables, parameters and the control variables are set up. The state variables are a function of the control variables and the state equations represent the system's behavior [Willigenburg, 2003]. The parameters are the constants in the system. The criterion is the cost function of the system, which has to be minimized for most systems. If the criterion is minimal, the control variables are optimal and the trajectory of state variables represents the optimal system behavior. As for the Euler-Lagrange equation, a minimum for the criterion does not guarantee to be the absolute minimum. It could be a local minimum. Unfortunately no conditions are known to distinguish global from local minima. In general, the only thing we can do is compare the function values of local minima and from them pick the one with lowest value [Willigenburg, 2003]. If different numbers of input lead to the same output, the probability of being the global minimum is high.

The variables in problems are related. These relations can be implemented as (in)equality constraints. Not only the relations between the variables are needed, also the derivatives with respect to the time or place are needed to solve the problem with optimal control. The derivatives are used to derive the neighboring points variables.

The problem is solved numerically, as stated above. All points are some distance away from the neighboring points. For all points the states and controls are considered to have initial values. These values are saved in a matrix for the state variables and a matrix for the control variables. In the rows are the different values for the different points in time or space and in the columns the different state or control variables. By setting the initial conditions in a proper way the minimization can be helped to search in the right domain. At one time this method derives all values in these matrices in the first iteration. In general, in optimal control problems an analytical solution does not exist and thus the solutions are obtained numerically [Lambregts, 1995]. The value for the states in points is determined with numerical integration. The control is described by Chebyshev polynomials. These mathematical functions will be explained below. When the state and control variables are derived, the criterion is computed and in the next iteration the programme looks for a lower value of the criterion. This calculation can be helped by setting the control variable in the proper domain. Next to the minimization of the criterion, the state and control output error with respect to the constraints is minimized. For every constraint this error should be small. The largest error is returned after every iteration. If the errors are small enough and the criterion is also minimized the result is said to have converged successfully and the optimal control is found!

The control variable controls the problem's state variables and so the criterion. The control has to be prescribed in a way to prevent an infinite number of output solutions. A parametrization with Chebyshev polynomials is an efficient way of parameterizing the control and it is a suitable numerical solution method [Willigenburg, 2003]. It is also possible to parameterize the states with Chebyshev polynomials. The parametrization can be compared to the parametrization of any function with Fourier series. The definition of a Chebyshev polynomial is stated in equation 3.18 [Lambregts, 1995]. The order zero polynomial is $H_0(s) = 1$, the first order polynomial is $H_1(s) = s$ and for $n = 2, 3, \ldots$ the higher ordered polynomials are defined in equation 3.18. For example the fifth order Chebyshev polynomial is $H_5(s) = 16s^5 - 20s^3 + 5s$. For a picture of the

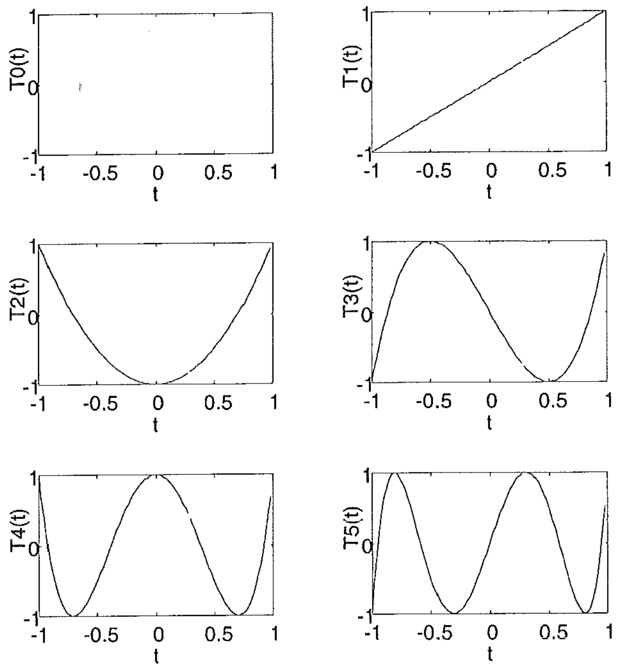

Figure 3.1: The Chebyshev polynomials up to order 5

Chebyshev polynomials up to the fifth order see figure 3.1.

$$H_n(s) = 2\,s\,H_{n-1}(s) \;-\; H_{n-2}(s) \tag{3.18}$$

To use the polynomials for control parametrization the time or space interval is shifted and scaled onto $[-1,1]$. Similar to Fourier series, any function of time or space can be approximated by adding a number of Chebyshev polynomials like in equation 3.19. The Chebyshev parameters $h_0, h_1, \ldots, h_{N-1}$ are called the Chebyshev coefficients.

$$f(s) \approx \sum_{n=0}^{N-1} h_n H_n(s) \tag{3.19}$$

The polynomials are orthogonal and every function can be described exactly by infinite Chebyshev series. These are advantages of the Chebyshev polynomials compared to other polynomials. Another advantage is that for a specific order of polynomials, the error of the Chebyshev polynomials with the parameterized function is lowest [Lambregts, 1995]. If the order is 6 for example, only $N = 7$ parameters have to be computed, but still the control can be approximated well. By setting the coefficients properly, every smooth function $f(s)$ can be approximated well. Especially for smooth problems this parametrization is good. The problem of finding the optimal meander's planform shape is smooth, because very sharp bends or sharp corners are not found for a meander in equilibrium state. All the derivatives of the state and control variables are continuous. A useful property of Chebyshev series is that Chebyshev series approximations of the s-coordinate can be related to Chebyshev series approximations of the derivative with respect to this s-coordinate. With this property the differential equation constraint of the control can be replaced by equality constraints on the Chebyshev coefficients of the control. Thereby time consuming numerical integration is avoided. When higher order Chebyshev polynomials are used, the accuracy improves at the expense of computation time [Willigenburg, 2003].

Chapter 4

Model description

4.1 Introduction

With the important theories for the derivation of the optimal meander planform shape stated, the model that is used to derive this optimal shape of the meander planform can be explained. The starting point is the flow model developed by Odgaard [1986a]. This model simulates the flow and bed topography in a meandering alluvial channel. It is summarized in the *dimensionless flow model and entropy production* section below. Because of geometric similarity, the model was made dimensionless by Teuling [2002]. In this dimensionless model, the total entropy production was implemented. Section *the optimal control problem formulation* explains how this total entropy production is minimized by converting it into an optimal control problem. In section *numerical solution* the computation method is described. Chebyshev polynomials are used to describe the curvature at the centerline. These polynomials are explained and finally the different possible outputs of the computations are explained.

4.2 Dimensionless flow model and entropy production

The flow model used to calculate velocity profiles in a meander bend of arbitrary shape was developed by Odgaard [1986a]. For a complete description of this model see Odgaard [1986a] and for applications of this model we refer to Odgaard [1986b] and Odgaard [1987]. The model is based on the solution of the equations for conservation of mass and momentum and the equation for lateral stability of the channel's bed. The equation of bed stability is linked to the momentum equations with a simple mass and flux balance. The net lateral transport of flow volume together with the mass and flux balance determines the streamwise variation of transverse bed slope. The main controlling parameters are the channel's width to depth ratio, the ratio of radius of curvature of the channel to width, the resistance characteristics and the sediment Froude number [Odgaard, 1986a].

The flow model has an analytical approach and is valid for steady, subcritical, turbulent flow in channels with uniform bed sediment. The longitudinal and transverse flow is derived at every point in longitudinal and transverse direction from surface to bed. This makes the model two dimensional. It should be noted that the stable meanders in this report can be considered to be in equilibrium state and thus are in steady state. The most important reason for choosing this flow model is that it is based on the same assumptions as the entropy production equation (equation 3.9) [Teuling, 2002]. Also for the entropy production equation the effects of banks on flow is considered to be insignificant. As a consequence the flow model applies to the effective width (w_e) [Odgaard, 1986a]. Other constraints of the Odgaard model are: (1) the channel width is constant; (2) the centerline radius of curvature is large compared to channel width; (3) the depth is small compared to the width; (4) cross-channel velocity components are small compared with down-channel components; and (5) the turbulence is isotropic [Odgaard, 1986a]. Isotropic turbulence means that the turbulence has the same magnitude in all directions at one point. This does not imply that the turbulence is homogeneous in the fluid, because the magnitude can be different everywhere in the fluid. These restrictions are satisfied for a shallow, moderately meandering channel with constant width.

Above it was shown that meandering is independent of scale. With this geometric similarity it is convenient to have a flow model that is independent of scale as well. The dimensions in the problem are time, length, mass and temperature. Since the entropy production will be written times temperature and per unit mass, only characteristic scales for length and time have to be defined [Teuling, 2002]. This can be done in the Odgaard model by dividing the velocities by the longitudinal velocity at the centerline averaged over the depth ($\bar{v_{sc}}$) and by dividing the length scales by the effective width (w_e). These variables are assumed constant in the flow model, which makes them appropriate for normalization. As an example the normalized transverse direction ($\tilde{n}$) and dimensionless longitudinal velocity ($\tilde{v_s}$) are derived in equation 4.1 and 4.2. In this report a tilde denotes dimensionless variables.

$$\tilde{n} = \frac{n}{w_e} \tag{4.1}$$

$$\tilde{v_s} = \frac{v_s}{\bar{v_{sc}}} \tag{4.2}$$

The characteristic timescale results from combining equations 4.1 and 4.2 [Teuling, 2002].

To determine the most probable meander planform shape the entropy production is minimized. Therefore the entropy production was implemented in the Odgaard model by Teuling [2002] and Andel [2002]. In appendix III taken from Teuling [2002] the Odgaard model is made dimensionless and the resulting model is summarized. This is slightly different from the Odgaard model [Teuling, 2002]. The most important equation in the dimensionless model is the equation that determines the transverse bedslope at the centerline:

$$\frac{\mathrm{d}^2 S_{Tc}}{\mathrm{d}\tilde{s}^2} + a' \frac{\mathrm{d}S_{Tc}}{\mathrm{d}\tilde{s}} + b' S_{Tc} = c' \, \tilde{c}_c \tag{4.3}$$

The parameters a', b' and c' are defined in appendix III. The parameters contain the dimensionless particle Froude number at the centerline (F_{Dc}) and the dimensionless velocity profile exponent (m). Although F_{Dc} and m are dimensionless, their value cannot be determined because the velocity profile exponent

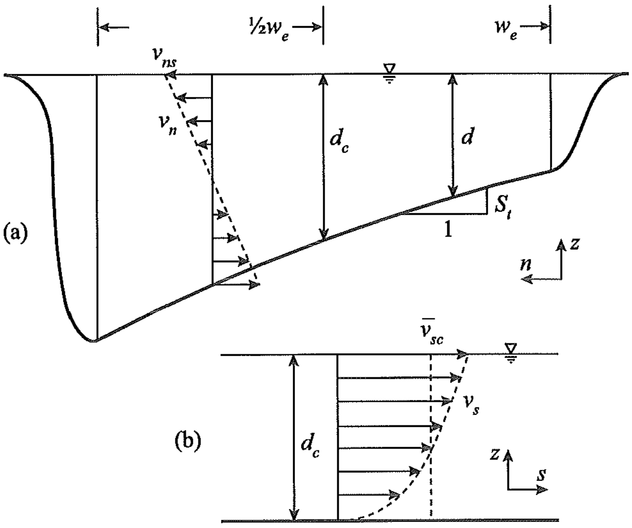

Figure 4.1: **A** Transverse velocity profiles in a cross section, transverse depth distribution and definition of model parameters; **B** longitudinal velocity profiles

is a function of the scale dependent Chézy coefficient and the particle Froude number is a function of the actual velocity and sediment size [Teuling, 2002]. However the scale dependent parameters have only small effect on the results [Teuling, 2002]. The values of the velocity profile exponent and the particle Froude number are taken as 2.8 and 6.78 respectively, the average values of the two river sites tested in Odgaard [1986b] [Teuling, 2002].

Equation 4.3 is a second order, inhomogeneous and ordinary differential equation. It is a forced and damped wave equation. The second term in this equation is the damping term and the term on the right hand side is the forcing term. The damping indicates that the system does not react instantly or in other words reflects the inertial forces of the system. The system is underdamped if $a'^2 < 4b'$, critically damped if $a'^2 = 4b'$ and overdamped if $a'^2 > 4b'$. If the system is underdamped, the system oscillates many times. If the system is critically damped, the system has one overshoot of the system's resting position at most [Vives, 2003]. If the system is overdamped the system only slowly returns to equilibrium, because of the strong damping term [Fowles and Cassiday, 1999]. For the values of F_{Dc} and m in the most usual range the system behavior is mostly underdamped [Vives, 2003].

A little further in appendix III, the depth distribution is clarified. The following statement is made by Teuling [2002]: "When interpreting S_T as $\mathrm{d}d/\mathrm{d}r$ this can be written for convenience as AIII-8." This follows from integration. The integration constant can be found by looking at the centerline. The equation then reads: $\ln d_c = \ln r_c^\gamma + C$, where γ denotes $\frac{S_{Tc} r_c}{d_c}$. This can only be satisfied if the integration constant (C) is set to be $\ln d_c - \ln r_c^\gamma$. Then equation AIII-8 follows from this integration constant. With the depth distribution known, the next step in the Odgaard model is to derive the velocity profiles. The result for the longitudinal velocity is equation 4.5 and for the transverse velocity equation 4.9. Examples of these velocity profiles are shown in figure 4.1 after Teuling

[2002].

With the velocity profiles derived in appendix III, the total entropy production equation (equation 3.9) can be simplified. The inner two integrals represent the entropy production in a cross section (σ_{cs}). The most inner or first integral of equation 3.9 can be solved analytically. Normalizing σ_{cs} by the temperature, density, effective width and averaged centerline longitudinal velocity, integrating and rearranging of terms yields (see appendix IV taken from Teuling [2002]):

$$\tilde{\sigma_{tot}} = \frac{T\sigma_{cs}w_e}{\rho v_{sc}^3} = \kappa^2 \int_0^{\tilde{L}} \int_{-\frac{1}{2}}^{\frac{1}{2}} \left(\frac{(m+1)^2}{4m^3 + 2m^4} \tilde{v}_s^3 + \frac{4\tilde{v}_s \tilde{v_{ns}}^2}{6m} \right) \mathrm{d}\tilde{n}\mathrm{d}\tilde{s} \tag{4.4}$$

The total dimensionless entropy production is now only dependent on the transverse surface velocity and the averaged centerline longitudinal velocity. Because no further analytical solution is available, this equation will be solved numerically. This is the equation to be minimized in order to derive the optimal planform shape of a meandering channel. One remark should be made about this minimization. The Odgaard model is made dimensionless and this implies that the longitudinal slope of the valley is not in the model anymore. The velocities are not dependent on the longitudinal slope, because they are normalized with the averaged centerline longitudinal velocity ($\tilde{v_{sc}}$). This makes that the lowest value for the total entropy production is found for a straight channel, where the path is minimized. In order to find a realistic solution, the model should have some constraint that makes the channel does not follow a straight line. For example the angle at the beginning and end of the channel can be set to some value that can be expected to occur in nature. Another example is to set the meander wavelength to the value usually found in nature (13.2 when normalized with the effective width).

4.3 The optimal control problem formulation

Finding the optimal meander planform is an optimal control problem where the planform is the control, the channel flow is the dynamic system and entropy production is the criterion to be minimized by the control. The dynamic system is described in the previous section. This is programmed in the sysmean-file (see appendix VI). This file is different for every optimal control problem. Together with the other files that describe the optimal control problem, it is called the programme in this report.

Normally in optimal control problems the state variables are denoted by x, the control by u and the time by t. For this study, the time was replaced by the longitudinal length without any problem, because we deal with a system in steady state. The problem only has 1 control input and the optimal control is expected to be smooth. Because the problem is smooth, the curvature or control is set between control bounds with inequality constraints. Another special property of this problem is that it is periodical.

A requirement for the programme are the differential equations for every state with respect to $\tilde{s}$. The states 1 to nx-6 (see appendix VI) refer to the square of the longitudinal velocities averaged over the depth ($\tilde{v}_s^2$) at points with the transverse coordinate from -0.5 to 0.5. Here, nx is set to 22, so the transverse discretisation steps are 1/15 w_e. Their relation with the control and bed slope is:

$$\frac{\mathrm{d}\bar{\tilde{v}}_s^2}{\mathrm{d}\tilde{s}} = -g'\frac{\tilde{d}_c}{\tilde{d}}\bar{\tilde{v}}_s^2 + g'\frac{\tilde{c}}{\tilde{c}_c} \tag{4.5}$$

In this equation the depth and the curvature are related to their centerline values. Thus these relations are substituted:

$$\frac{\tilde{d}}{\tilde{d}_c} = \left(\frac{\tilde{c}_c}{\tilde{c}}\right)^{\frac{S_{Tc}}{\tilde{d}_c\tilde{c}_c}} \tag{4.6}$$

$$\frac{\tilde{c}}{\tilde{c}_c} = \frac{1}{1-\tilde{n}\tilde{c}_c} \tag{4.7}$$

The resulting equation is programmed for every transverse point in the first lines of the system dynamics. The sign function and the maximum of the control and epsi are used to prevent the programme from dividing by zero. The second state is the transverse bedslope at the centerline. This is described by the second order differential equation 4.3. Because it is a second order relation, also the first differential with respect to $\tilde{s}$ is a state variable. This is the third state, nx-4. The next state represents the angle β (see figure 2.1). The derivative of this angle with respect to the longitudinal coordinate is minus the curvature at the centerline:

$$\frac{\mathrm{d}\beta}{\mathrm{d}\tilde{s}} = -\tilde{c}_c \tag{4.8}$$

With this angle derived, the X-coordinate and Y-coordinate can easily be obtained by adding the sine and cosine of this angle to the previous steps, respectively. Consequently the resulting planform shape can be drawn in usual Cartesian (X,Y)-coordinates. With the X-coordinate value at the end of the channel, the wavelength of the meander is known. The last state is the criterion that has to be minimized (equation 4.4. Because the flow velocity at the centerlines surface in the transverse direction ($\tilde{v_{ns}}$) is only needed to derive this criterion, the $\tilde{v_{ns}}$ is defined only here in the programme. Its relation with the states and control results from:

$$\tilde{v_{ns}} = d'\,S_{Tc}\frac{\tilde{d}}{\tilde{d}_c}\frac{\tilde{c}}{\tilde{c}_c} \tag{4.9}$$

In the programme the relations 4.6 and 4.7 are substituted in equation 4.9. This transverse flow velocity at the centerlines surface is used together with the longitudinal velocity averaged over the depth ($\bar{\tilde{v}}_s$) to derive the criterion.

The parameter vector includes all constants in the programme. The first three parameters are a', b' and c' in equation 4.3. The fourth is the g' in equation AIII-10. The fifth is the depth at the centerline. The sixth and seventh parameters are needed to derive the criterion or total entropy production. They are the first and second fractions without flow velocities in equation 4.4, respectively. The last parameter is the d' in AIII-12. For this the particle Froude number is taken to be the particle Froude number at the centerline.

To have realistic solutions for $\bar{\tilde{v}}_s^2$, a state inequality constraint was implemented to have only positive values. Because only one period of a meandering channel is derived in this programme and the process is assumed to be periodical, all state variables and the control variable except for the criterion and the X-coordinate have to be equal at the beginning and end of this period. In fact, all derivatives with respect to the longitudinal coordinate should be equal at the beginning and end. The first derivative is set equal at beginning and end in comments. Furthermore a terminal state constraint was set on the Y-coordinate to make sure the channel flows in valley direction. A terminal constraint on the X-coordinate to end around 13.2 was attempted, but could not be satisfied.

The initial conditions for the states and control were optimized in this problem, except for the angle β in most runs. This was set to some value to find a downvalley flowing channel with some sinuosity.

4.4 Numerical solution

The optimal control problem is programmed in matlab consisting of several files. Because the optimal control software call the optimization command FMINCON, a matlab version with optimization toolbox is needed. On top of every file is an explanation about the arguments in brackets. The input files or variables and the output are explained.

To start the calculations the Tcmr-file is called (see appendix V). At first the matlab workspace is cleared and the constants in the meander model are defined in the parameter vector. The next step in the file is to set the tolerance on the computation. After this the file optchebi is called. This file parameterizes the control ($\tilde{c_c}$) with Chebyshev polynomials. The states are derived by numerical integration. This is done by the function ODE45 in matlab. Further the longitudinal coordinate (0 to $\tilde{L}$) is scaled onto the range of the Chebyshev polynomials $[-1, 1]$. The arguments of the optchebi-file are stated in brackets following the file-name optchebi.

The sysmeanfinal file is the system file that will be used. The empty argument is the startname, which is an easy option to use former calculations for input. Mr20 is the optname, which is the output of the programme with extension mat. In this mat-file the optimal values for the matrices are saved for the best solution, if the calculation ended successfully. The fourth argument is the order of Chebyshev polynomials used. In the Tcmr-file added this order is set to 6 and in comments the same calculation is repeated with an order of 12 and with input from the first calculation. The fifth argument can be used to set the number of longitudinal points. In this run the longitudinal discretisation steps are set to 1/99 $\tilde{L}$, which makes 100 longitudinal points. The sixth and seventh argument are defined just above the calling of optchebi. With the options argument different calculation options can be set. The last argument is the parameter vector stated above. With these arguments the optchebi-file generates a vector bopt. In this vector the coefficients of the Chebyshev polynomial serie that parameterize the curvature at the centerline are generated. The number of coefficients is 1 plus the order, so in this case 7. In the first step an initial guess for the 7 coefficients is made that satisfies the constraints as good as possible. These initial values are improved every step by decreasing the error on the constraints and by looking for a lower value of the criterion. This is done by the function FMINCON. This minimization function has the files optchbco and optchbfi as input-files. In these files all relevant information is stored to solve the problem. When the computation succeeds the solution is saved in the mat-file and the file cheb2tmr displays the result.

Then the Lxu is integrated with the trapezoidal rule in the transverse direction by adding the different values of Lxu in one cross section. The first and the last value are thus only a half time in the equation. This is the most precise way of integrating numerically. Then out(nx,i) is the derivative of the criterion in longitudinal direction at every longitudinal point. It should be noted that in the programme the constant κ^2 in front of the integral in equation 4.4 is omitted. This has no effect on the control and state values found by minimizing the total entropy production. Just below the system dynamics in the sysmean-file, a safety line is programmed. If for some reason imaginary numbers do occur, a warning is given and the computation can be stopped. Something must be wrong in the programme, where only realistic values should be generated.

The next important lines in the sysmean-file are the constraints. For example the square of the longitudinal velocity averaged over the depth ($\bar{\tilde{v}}_s^2$) cannot be smaller than zero. Also, the curvature at the centerline is set in the range $[-0.5; 0.5]$ and in comments (not used in the calculations) the value of the X-coordinate at the end point is set around 13.2. A little further the initial conditions for the first longitudinal point are stated. The state variables defined in the vector pa are only to start the computation with at the first longitudinal point. For the squared longitudinal velocity averaged over the depth ($\bar{\tilde{v}}_s^2$), the initial values for the points in $\tilde{n}$-direction from -0.5 to 0.5 are taken to be $cos^2(2\pi\tilde{n})$. For the transverse bedslope and the derivative with respect to $\tilde{s}$, the initial value is taken for an imaginary negative sine-generated curve. Consequently, the curvature of this negative sine-generated curve is positive in the beginning and the derivative is negative. The values in the vector pa are optimized in the programme to the value where the criterion is lowest. In this case only the angle β is a hard constraint. This value cannot be optimized and is the same at the end and beginning. This is programmed in the final conditions, where also the Y-coordinate is set to 0. This forces the X-coordinate at the final longitudinal point to be the wavelength of the meandering channel. Further the end time (or the longitudinal length in this study) can be set to be free or fixed. In this case it is fixed to the value Sf, defined to be 39.6 on top of the file.

An alternative for the use of optchebi is the file optcheb. This file parameterizes both states and control with Chebyshev polynomials, which makes the calculation computationally faster, but less accurate. Aopt is derived by the file cheby. The file cheb2t compares the final result of the states with the states generated by numerical integration. The difference is generated as output with the name dynamic error. Not surprisingly, this difference should be small. It should be noted that the Chebyshev polynomials in the range of -1 to 1 are either equal at the end (even orders) or they have the same differential with respect to the longitudinal coordinate at end and beginning (odd orders). Both should be equal to have a real meandering river, which is not the case for any order of Chebyshev polynomials.

The returned output by the programme is in the matlab command window. If the programme is programmed correctly, the calculations start by calling the Tcmr-file. During the calculation for every iteration, the error with respect to the constraints, the criterion and the procedure followed is a line of output. The programme minimizes the error and the criterion. When the calculation is finished, the optchebi-file checks if the solution is feasible. This is done by comparing the final output with tolerances stated. If the solution is feasible, a good solution is found and the computation stops by itself. The other possibility for matlab to stop the calculation is when the maximum number of function evaluations is exceeded. This number can be set in the file optchebi under options MaxFunEvals. The iteration with minimal error on the constraints is the best solution to the problem. Finally, this value is written in the output together with the value of the criterion.

Chapter 5

Results

In the previous chapter, the model was described. Runs of this dimensionless model, with the Odgaard flow model and the entropy production equation embedded in the optimal control problem, are presented in this chapter. One result of the model approximates a natural, stabilized meandering channel. This planform shape comes close to the empirical relations stated in section 2.2. First, this result will be described. After that, the attempts made to achieve more results with an expected shape of meander planform will be summarized and some results will be given additionally.

The best result obtained in this research is shown in figure 5.1. This figure shows that the wavelength of the meander is around 13.2 (actual value is 13.658) and the amplitudes of both bends are in the same order of magnitude. These are results that are expected for a natural, stabilized meandering channel. The result is achieved with the hard constraint on the angle β to be at beginning and end 1.2π and meander length ($\tilde{L}$) 39.6, which implies a sinuosity of three. Initial values for the transverse bedslope and its derivative with respect to longitudinal length were given (-0.03 and 0.015 respectively), but after optimization these values differ largely from these initial values (-0.18609 and 0.24874). The initial values of the dimensionless, squared, longitudinal, averaged velocity at the transverse points are set to be $cos^2(2\pi n)$. The constants a', b' and c' in equation 4.3 and the constants in equation 4.4 were determined using $\kappa = 0.4$, $m = 2.8$, $\alpha = 1.27$ (as for ordinary river sand), $F_{Dc} = 6.78$ and $\theta' = 0.27$. The order of polygons that describe the control is set to 6.

It is important to realize that the inflection point does not have to be at the X-axis. Partly because the beginning of the channel is arbitrary determined to be 0 for the X and Y coordinates and partly because the inflection point may be delayed. Figure 5.1 shows some unexpected characteristics as well: the second bend is much wider than the first bend in the figure; and the skewing is not upstream as expected, but the maxima and minima appear to be shifted in downstream direction, in the positive X-direction. This planform shape is derived from optimizing the control, the curvature. This is shown in the last graph in figure 5.2, titled u1. The X-axis in these graphs represents the longitudinal length. This last graph shows that the curvature is positive in the first part, negative after the first inflection point and after the second inflection point it is positive again. The maximum and minimum curvature are both around $(-)0.3$. Unexpected is that no symmetry in the positive and negative parts of the graph

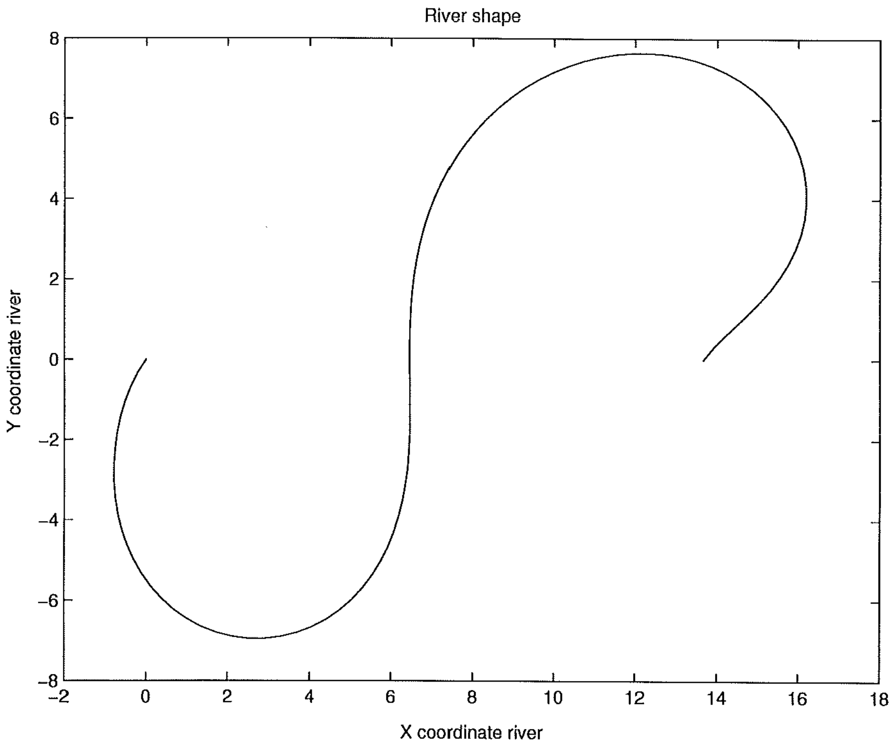

Figure 5.1: The planform shape resulting from a model run with a sinuosity of 3 and β fixed to be 1.2π at beginning and end of the meander period.

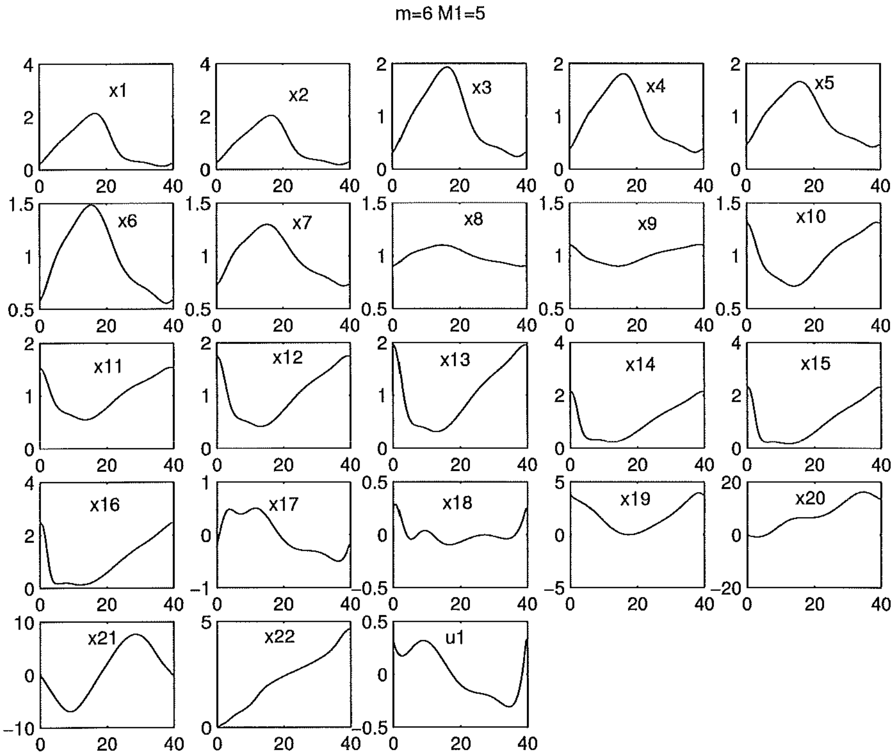

Figure 5.2: The states and control for the result with a sinuosity of 3 and β fixed at 1.2π at beginning and end of the meander period.

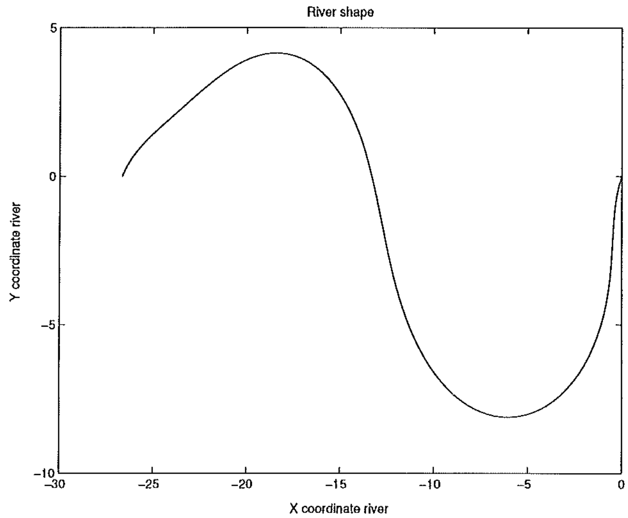

Figure 5.3: The planform shape resulting from a model run with a sinuosity of 3 and β fixed to be 1.17π at beginning and end of the meander period.

can be seen for $\tilde{v}_s^2$ and S_{Tc}. The values at transverse points of $\tilde{v}_s^2$ are steep in the first bend and not so steep in the second.

The other graphs in figure 5.2 represent the states of the problem. State x1 to x16 are the squared, dimensionless, longitudinal velocities averaged over the depth ($\tilde{v}_s^2$) from the effective right side of the channel to the effective left side. The distance from the point where x1 is taken to the point where x16 is taken is thus 1 effective width. x8 and x9 are in the middle of the channel and here the amplitude of the $\tilde{v}_s^2$ is lowest. The maxima are in the middle for the first 8 points and in the beginning and end for the last eight lateral points. Also the maxima and minima increase going in outward direction. Graph x17 represents the transverse bedslope at the centerline. It shows periodicity and the maximum and minimum are a little delayed after those of the curvature. The amplitude of both maximum and minimum is about 0.5. Further, more than one minimum and maximum is present. The next state is the derivative of the transverse bedslope in longitudinal direction. It can be deduced from the transverse bedslope. x19 represents the angle β. It starts and ends at 1.2π and is negative in four points in the middle of the channel. At these longitudinal points, the channel flows in negative direction of the X-axis or upwards in the valley. For the control and all states mentioned so far, the values at beginning and end are the same. This is due to the equality and end constraints. For β this implies that the first derivative with respect to s is also the same, because of the relation with the curvature. The states x19 and x20 are the X and Y lengths respectively. Together they result in figure 5.1. The last state is the entropy production. It increases not completely linear to a value of 4.6483.

Because this result is promising, attempts have been made to find more results like the one described above. When the angle was increased with 0.005π, the X-coordinate at the end point increased largely and thus the wavelength was too long to be realistic. All input parameters were held constant, only

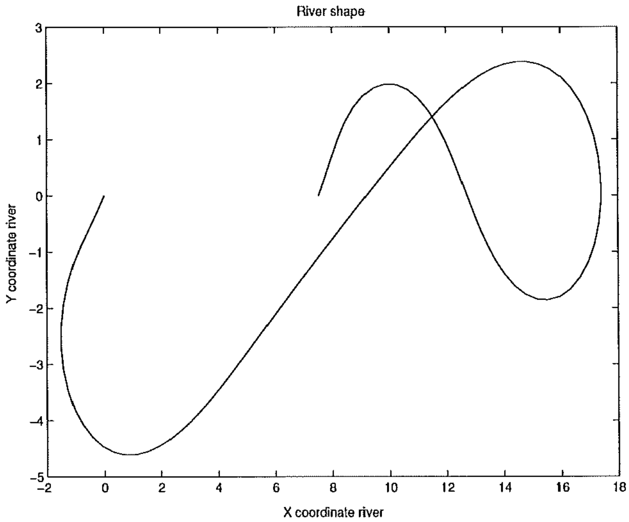

Figure 5.4: The planform shape resulting from a model run with a sinuosity of 3 and β fixed to be 1.21π at beginning and end of the meander period.

the hard constraint β was changed. When it was changed to 1.17π (see figure 5.3), 1.202π and 1.25π, this resulted for all three runs in a channel flowing in upvalley direction. To overcome this error, the angle β was set to be maximal 4 with an inequality constraint. Every value for the starting angle (even 1.2π) with this inequality constraint did terminate the optimization. Apparently this constraint is too strong for the optimization programme.

Another attempt was to increase the angle β to 1.21π. This resulted in figure 5.4. This result shows a strange cut-off, not known for meandering channels.

The results gathered from the changes in the angle β show that the non-linear model is very sensitive for this hard constraint. Only a small change in angle, results in a completely different planform shape. The result for $\beta = 1.2\pi$ is a lucky hit! It would be satisfactory not to try different angles, but to have a constraint on the model that restricts the wavelength of one meander bend in a range around 13.2. This constraint was implemented as hard inequality constraint (see appendix VI in comments). The range is arbitrarily chosen to be -1 and +1 from 13.2. Consequently the angle β could be optimized freely. Many runs have been made, but an error occurred on every run and no solution was obtained. The errors were amongst others: search direction is less than 2 times options.tolX, but constraints not satisfied; no feasible solution found, no convergence. This was not only tried for a sinuosity of 3 with the good result as input, but also for a channel length of 26.4 (so a successful result would have sinuosity 2). The problem seems to fulfill the equality constraints together with this constraint.

Because it is believed that the stable meandering planform shape is repeated for every period, an extra constraint on the derivatives of the states x1 to x19 and the control was implemented. Not only the value at beginning and end have to be the same for an iterative system, but also all derivatives with respect to s. The first derivative is set equal at the first and last point for these variables.

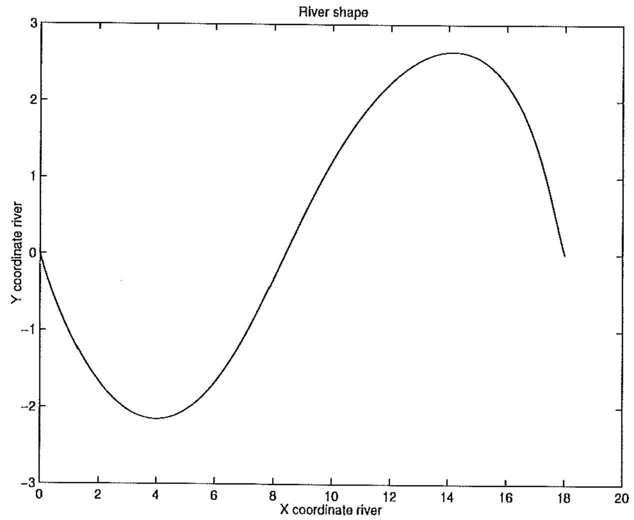

Figure 5.5: The planform shape resulting from a model run with a sinuosity of 1.6 and β fixed to be 0.8π at beginning and end of the meander period.

Runs did not lead to results, probably because the constraint was too strong. Even for only one variable with this constraint, no solution was obtained.

Another variation in the good result is to lengthen the longitudinal length. Then a non-iterative system can be found and possibly a meandering system is slightly different in every bend dependent on the initial conditions of the bend. With this assumption, no constraints have to be met concerning the begin and end points of a meander period. The longitudinal length was increased to 118.8 and to 200, but both runs resulted only in a longer computation time, a higher maximum error and a higher value for the criterion. No periodic behavior was found.

The most runs have been made with an expected sinuosity of three, but also other values have been tried. The longitudinal length was set to 21.12, which resulted in figures 5.5 and 5.6. It can be seen that the meander wavelength is far above the expected range. The solution is not enough curved or the channel is too linear. Attempts to use increased angles as constraint, did not lead to a solution. If a solution was found, often all squared, dimensionless, longitudinal velocities averaged over the depth ($\bar{v}_s^2$) evolved to a value of one exponentially and in the end part of the period, the $\bar{v}_s^2$ remained one constantly. For a longitudinal length slightly higher, the model output was almost straight. The length was set to 21.2 and a completely different planform shape resulted. This can also be due to the lower order of Chebyshev polynomials used to describe the control: order three in stead of six. In an other attempt this order was increased to 12. The computation time increased, but the good result obtained with order six was not changed obviously.

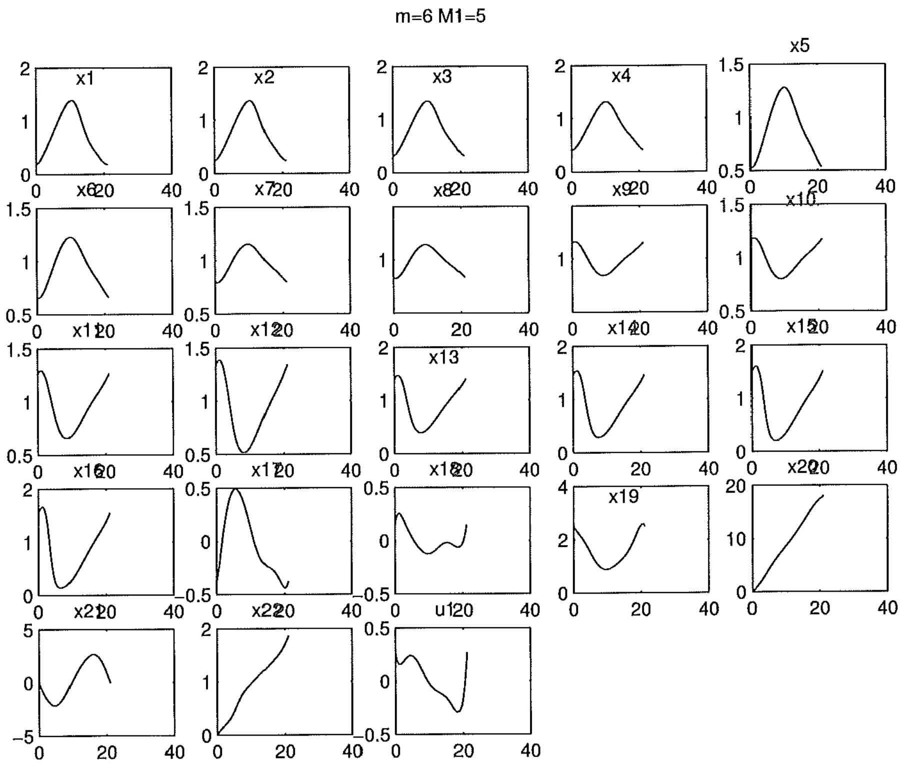

Figure 5.6: The states and control for the result with a sinuosity of 1.6 and β fixed at 0.8π at beginning and end of the meander period.

Chapter 6

Discussion

6.1 A comparison with planform shape found in nature

The stable, natural meander planform shape can be derived from minimizing the total entropy production of an open alluvial channel reach with homogeneous meandering characteristics for a given sinuosity. To predict this sinuosity is difficult, if not impossible, because variables that influence the sinuosity are interrelated and have different impacts in different channels. In this study a dimensionless meander model has been formulated as an optimal control problem. For a given sinuosity the optimal planform shape can be derived. Because no restrictions on the resulting planform shape are implemented in this model, both the asymmetric downchannel delay of the inflection point and the upvalley skew asymmetry can be found, as well as the fattening with respect to a first order sine-generated curve. The downchannel delay of the inflection point cannot be found with the assumption on the planform shape to be a third order sine-generated curve. At least one result with sinuosity 3 is promising. It shows typical characteristics of the meander planform shape: the meander wavelength around 13.2, an expected velocity profile and both bends having the same order of amplitude in control and states. But not all constraints that should be satisfied to describe a natural alluvial meander, could be implemented in the optimal control problem successfully. For the promising result, the states and control are not periodical and the upper bend differs considerably from the lower bend. This may be, because the result does not satisfy all the constraints to make it a periodical meander. The planform shape derived in this study is thus not a final result. For this reason the correspondence of the resulting meanders from this model with natural meanders found in nature is not further investigated.

The question may arise, whether the stable meanders derived in this study do exist in nature. For the modelling in this study it is assumed that the meandering channel is stationary, has homogeneous sediment and is regularly (shows periodicity). This ideal, stable characteristics are seldom found, because of the constantly changing boundary conditions in nature. But in nature meandering channels are likely to evolve towards an equilibrium planform shape. This is in the stable state of the meandering process in the theory of Stølum [1996]. The planform shape in this stable state seems to be independent on bed material, vegetation or changes in discharge. These variables only affect the length of time, at which the equilibrium state will be reached. The existence of these stabilized meanders appears at topographical maps of places, where man do not influence the meandering channel. In figure 7 of the extended version by Teuling [2002], 24 stable river bends with one complete wavelength are redrawn after topographical maps. Nice extended regular meander systems can be found in the tectonically stable Precambrian shield areas like the Amazon basin. The assumption of periodicity is also made by for example Carson and Lapointe [1983], Edwards and Smith [2002], Hey [1976], Ikeda et al. [1981] and Parker et al. [1983]. This strengthens the assumption that the optimal planform shape of meanders shows periodicity. On the other hand, most river reaches do not show this regularity. Following bends are slightly different shaped, partially caused by different external conditions or changes in downvalley directions. Another reason might be that different meander bends have slightly different initial conditions and consequently a different planform shape. Because the system is non-linear, the solution is extremely sensitive for only small changes in initial conditions as shown in the results. Some models describe the meander planform without using the assumption of periodicity, for example Lancaster and Bras [2002], Liverpool and Edwards [1995], Stølum [1996] and Stølum [1998]. Possibly, the process of meandering is chaotic and best described by the Lorentz chaotic principle. Then no conclusion can be drawn from the planform shapes of one meander period derived in this study, because the initial conditions determine the final result to a large extend.

For larger rivers natural, free meanders can only be found in more remote areas. Brooks and streams show the natural meandering pattern more often, because changes in planform are faster than in rivers. The transition from active to stable meanders and the other way round is more rapidly. This also implies that a smaller channel is more susceptible to changes in flow or sediment conditions. For example, when the discharge is high for some period, the channel adjusts to this discharge and is likely to be in the active state, changing its planform shape. Because the planform shape adjusts to the conditions more easily, the stream or brook will be in the stable state faster than a cumbersome river. Consequently, for a river the time in the stable state will be longer and may be up to hundreds of years.

6.2 Dimensionless flow model and entropy production

The flow in meandering channels is approximated in this study with the Odgaard model. This model strongly simplifies the flow pattern and is only valid for steady, subcritical, turbulent flow in channels with uniform bed sediment. The flow is modelled to be 2 dimensional. Secondary flow is implemented in the model and the resulting transverse velocity is assumed to be linearly related with the depth in the channel. The Odgaard model applies to shallow, moderately meandering alluvial channels with constant width. Near the banks, where a vertical flow is expected because of the secondary flow, flow velocities are not derived. The model applies only to the effective width of the channel, where no bankflow occurs. On the contrary, in the deterministic model of Ikeda et al.

[1981] the difference between flow near the bank and the average longitudinal velocity determines to a large extend the bank retreat and thus the planform shape. Furthermore, the friction factor is taken to be constant in the Odgaard model. Silva [1999] points out that the friction factor is not only dependent on channel roughness, but also on position and sinuosity. Vertically averaged flows for two test sites can only be explained with a changing friction factor.

Because only small changes in flow velocities can cause large changes in planform shape, simplifications in the flow can result in unrealistic solutions of the model. Therefore it could be satisfactory to derive the optimal planform shape from more sophisticated models, for example Delft 3D. But for this model the stresses should be known on forehand, so also assumptions that will affect the resulting planform shape have to be made. Furthermore, the Odgaard model is successfully tested for a sequence of sine-generated curves. The simulated flow and bed features are in good agreement with a data set of a field study without the use of calibration factors [Odgaard, 1986b]. This proves that the simplifications made are reasonable and physically acceptable [Odgaard, 1986b]. The model could provide input to general analysis of meander patterns [Chang, 1984].

The assumption in the Odgaard model that the radius of curvature is large compared to the width, is not satisfied for higher sinuosities. Then high curvatures are present in the planform and the assumptions about the flow pattern are not valid anymore. These sharp bends have been shown to be likely to evolve to a stable state with the deterministic approach. If the transverse velocity at the border of the channel does not increase in the entire depth as assumed in the Odgaard model, but decreases at some depths with higher vertical place, two flow cells that converge away from the outer bend are present [pers. comm. K. Blanckaert, 2003]. These cells protect the outer bend from erosion by the main flow.

In the model set up in this study, the relation between the meander wavelength and the width is taken to be linear. In fact, Leopold et al. [1964] found that the meander wavelength is proportional to the width to a power 1.01. This simplification in making the model dimensionless does not influence the end result to a large extend. For a comparison of a 100 meter wide river and a 4 meter wide brook, the error between modelled and real meander wavelength is not larger than 5 %. Additionally, if this model is used for deriving the shape of a meander planform, the meander wavelength can be set to the meander's dimension easily.

In the Odgaard flow model, the total entropy production was implemented. To set up an equation for this entropy production, assumptions are made. These assumptions are the same as made for the Odgaard model, which have been discussed above. The assumption to neglect flow influenced by the bank, seems to be a rough estimate. Near the banks the friction with the bed is high and as a result entropy is produced. But in Hooke [1975] it is explained that it is not the bed shear stress that governs the entropy production, but the internal shear stress. This makes this assumption much better.

The minimization of entropy production is an extremal hypothesis. These statements are criticized, because they do not have the explaining power that deterministic derivations have and because the thermodynamical statements used are strictly not valid for non-linear and open thermodynamic systems. But in section 3.2 the validity of the entropy production minimization in open, non-linear systems is strengthened with the theory of Reiser [1998, 2000, 2001, 2003]. Another argument in favor of the minimization is that meanders are not restricted to the presence of sediment. Meanders can be found in many fluid flows and some general law should prescribe the equilibrium state of the meander planform shape. It is proposed that this law is minimization of entropy production. For complex problems, a solution can be obtained more easily using the principle in stead of solving the momentum equations. In general, the tendency towards minimization of entropy production can be used to solve many complex chemical and physical problems.

The flow model with the entropy production equation was made dimensionless. This is satisfactory, because the process of meandering is independent on scale. Two variables in the flow model are dimensionless, but their value cannot be determined. These are the particle Froude number, which is a function of the actual velocity and sediment size, and the velocity profile exponent, which is a function of the scale dependent Chézy coefficient. They have been set to the average values in the two test sites in Odgaard [1986b]. Teuling [2002] performed a sensitivity test on these flow and sediment parameters and they seem not to influence the flow pattern and resulting planform shape to a large extend. This test was performed with the assumption of third order sine-generated function, but probably the conclusion is also valid for the optimal planform shape derivation in this study.

6.3 The optimal control problem formulation

The problem of finding the optimal planform shape of an alluvial meander was formulated as an optimal control problem. The control and states for this three dimensional system were derived using numerical integration. In general, this is assumed to be a precise way of integration also for non-linear models, but possibly errors are generated. A spatial discretisation is required which should be sufficiently accurate.

Inherent to minimizing some function, is that solutions obtained can be local minima. In this model, attempts have been made to find the solution with the global minimal total entropy production, but it is never definite that this minimum is found. The good result found for the hard constraint on the starting angle 1.2π appeared to be independent on the initial conditions. It is likely that this result is indeed a global minimum of the total entropy production.

The control or curvature was parameterized with Chebyshev polynomials. These polynomials are efficient to use, because only small order can make a large range of curves. With a run of the model with the order only three, the resulting planform shape did show some simplifications. Another run with order 12 did result in a similar solution with the solution obtained with order 6, therefore it can be concluded that the order 6 is indeed sufficient, as expected for smooth problems.

In this study the assumption was made that a meander shows periodicity. Because Chebyshev polynomials are not restricted to periodic behavior, constraints had to be implemented to end up with realistic, regular solutions. Chebyshev polynomials of some order have either the value or the first derivative equal at beginning and end. So a combination of orders has to made to satisfy both constraints. At least two even or two odd orders are needed to satisfy both these constraints. The constraints that the first derivatives of the states and control with respect to the longitudinal coordinate should be equal at beginning and end of the meander period are not satisfied for the good result. The freedom to optimize the coefficients is largely restricted. When even higher derivatives are set equal at beginning and end, this freedom becomes very small and it is likely that no solution can be obtained that satisfies these additional constraints. Nevertheless, the good result shows that the planform shape and the states are more or less periodical, but the solution still has to be improved.

A remark can be made about the calculation process. Although constraints were implemented to find realistic solutions, during calculations the path of the curvature or states can be unrealistic. The assumptions made when setting up the model (for example that the channel is moderately meandering), do not have to be satisfied for all iterations. As long as the final result of a calculation is realistic and does satisfy the constraints, this problem is unimportant. Moreover, when a run is performed with for example the good result as input, the constraints are likely to be satisfied for all iterations if the end result does satisfy them as well. For the curvature this error can not be large: a constraint was implemented that it is in the range from -0.5 to 0.5. Values out of this range denote too sharp bends and are unrealistic.

If the calculation succeeded to find a meander planform shape resulting in minimization of total entropy production, a solution of the model was obtained. Only one solution was in the range of the meander length around 13.2. For this good solution the final point has (X,Y)-coordinates: $(13.658; -0.0006358)$. A constraint on the Y-coordinate was implemented to be around 0, because the definition of the angle β is that it is the angle of the transverse direction of the centerline with the negative X-axis (see figure 2.1). Consequently the meander wavelength could be read from the end value of the X-coordinate directly. Maybe this constraint is too strong and it is not very necessary to be exactly 0. The range of the final Y-coordinate can be set a little wider. As a result, other more important constraints can be satisfied possibly.

It was found that the end result is very sensitive on the hard constraint that the angle is set at beginning and end. For a sinuosity of three, this angle was calculated to be around this value. Then the channel flows upvalley in small parts of the reach, which is also seen in nature for this sinuosity. The solution did end in the range around 13.2: the expected wavelength. But when the angle was only increased or decreased with small steps, the resulting planform was completely different. The good result is a lucky hit!

Also the sensitivity on the discretisation in both n and s direction has been investigated. Both discretisations were increased. The computation time increased up to 3 hours, but the result did not show considerable differences with results derived with lower discretisation. Thus for the s-direction a discretisation of 100 points and for the n-direction of 16 points seem to be sufficient for deriving the first solutions of the problem.

Chapter 7

Recommendations

7.1 Dimensionless flow model and entropy production

In the previous chapter, the results obtained with the optimal control problem were discussed and some recommendations for future research follow directly from this discussion. A first recommendation is about the flow model (see section 6.2). When a final result is obtained with the dimensionless Odgaard model with the total entropy production implemented, it is wise to use another (more sophisticated) flow model to test if the assumptions made about the flow pattern in the Odgaard flow model do not influence the resulting planform shape. If the Odgaard model does not approximate the flow well, the entropy production cannot be derived with the assumptions made in the flow model as well.

Another test that should be performed is a sensitivity test on all input parameters. Especially those parameters, that were assumed to have values measured in only a few practical studies and are related to actual, non-dimensionless velocities, sediment size and Chézy coefficient, need to be checked on their range of validity. Although Teuling [2002] performed such a test for the particle Froude number and the velocity profile exponent, this test should be repeated when a final result is obtained with the model set up in this study. Because no assumptions that prescribe the planform are made, the sensitivity of the model output on these parameters can be different in this study. Another parameter that needs a sensitivity test is the ratio of width to depth at the centerline. To complete the testing of input parameters, the constants in the equation for the transverse bed slope at the centerline can be tested as well. This is for the Shields parameter and the ratio α.

Although the extension of the statement of Prigogine to non-linear and open systems is strengthened in this report, the validity of this principle of minimal entropy production needs to be further investigated. The assumptions used to derive this extended law should be tested and the validity of the application of the general fourth main law introduced by Reiser [1998] on turbulent meandering flow should be investigated.

7.2 The optimal control problem formulation

In the good result the necessary states and control are equal at beginning and end. Attempts were made to set the first derivative with respect to the longitudinal coordinate equal at the beginning and end, but this has not resulted in solutions yet. Only the simplest way of implementing was tried. Other ways of implementing the constraints in the variational procedures should be tried. Probably the result will improve considerably when the first derivatives are equal, but actually all derivatives must be equal at beginning and end of the meander period to have a periodical meander planform shape. All these constraints can probably not be satisfied at once.

An alternative for the parametrization of the control with Chebyshev polynomials is a parametrization of the curvature with Fourier series. These are periodical functions and thus they satisfy the continuity constraints by definition. The third order sine-generated curve used by Teuling [2002] to describe the planform shape is a Fourier serie, but this is not able to describe the delayed inflection point asymmetry in the planform shape. This asymmetry can be found additionally, when higher orders of Fourier series are used. The planform shape is the result from the control and thus it is believed that also higher orders Fourier series have to be used to parameterize the control. With a fifth order parametrization of the curvature the delayed inflection point can probably be found, but maybe higher orders are needed to describe the resulting planform shape with delayed inflection good. This parametrization leaves more freedom to find the optimal solution, because no constraints have to be satisfied to describe periodical behavior.

The good result with the constraint on the angle β to be 1.2π at the beginning and end, is a lucky hit. The range of this angle with realistic end results needs to be further explored. This can be done by trying angles and see what is the result. If several solutions are found, it could be useful to combine them and see whether combinations of these solutions represent planform shapes as well. An algorithm that could be useful then, is the genetic algorithm. It combines solutions and sometimes strange solutions as well, to make an overview of the range of solutions. As only the global minimum is of interest, the lowest minimum can be chosen to be the best planform shape for the given sinuosity. In this study only one good result was found for sinuosity three. For other sinuosities a search for realistic solutions should be performed as well. Change the meander length and consequently the constraint on β and run the model!

Another algorithm that helps to find the global minimum is simulated annealing. It is a powerful stochastic search algorithm applicable to a wide range of problems for which little prior knowledge is available. It is likely to converge to the global optimum by making large and small steps. Other algorithms decrease their stepsize when the solution is close to a local minimum and are likely to find the local minimum to be the solution. With this algorithm the probability for the solution to be global is higher.

Not only algorithms, also data from field sites can be helpful in finding the global minimum. When stabilized, regular, alluvial meander planform shapes are used for input of the model, the end result should be similar with the input. This is a good test for the model assumptions and of the models ability to find the global minimum.

Some tests have been performed to test the sensitivity. The discretisation and order of Chebyshev polynomials seemed to be sufficient, but when a final result is obtained, these tests should be repeated. It could be that for this final result the sensitivity is different or deviations are more clear.

The assumption made in this study that the meandering process shows periodical behavior, does not have to be right. The high sensitivity on the constraint about β is an indication that the system is chaotic. Very slight changes in initial conditions for every bend, can result in different planform shapes. To test this hypothesis, the parametrization of the curvature with Chebyshev polynomials is good. For a large number of bends the optimal planform shape can be derived. To do this the meander length should be set to $n \cdot 39.6$ to result in a meandering channel with sinuosity three. A complication is that either the constraint on β or a constraint on meander wavelength has to be satisfied to end up with realistic planform shapes. The best would be to implement a constraint that forces the end point to have coordinates around $(n \cdot 13.2, 0)$. It might help to decrease the discretisations to save computation time.

This optimal control problem formulation can also be used for a model with dimensions, for example the model of Andel [2002]. Then no constraint has to be implemented to force the channel to meander. With this model, the optimal sinuosity and planform shape could be derived for a site in nature with parameter values and constants measured at this site. These can be interpreted as the optimal characteristics of the channel in the ordered state after the channel has evolved to steady state.

7.3 Final remarks

In this section I would like to make some final remarks, that do not consider alluvial meandering channels.

Surface tension meanders can be created in the laboratory. A problem arises, when determining the cross-sectional shape of these meander flows. When two parallel inclined plates are used, the cross sectional shape can probably described and measured easier. The contact angle with the two glass plates possibly can be set to be linear and the contact angle is no longer dependent on the centrifugal force. Interesting is what sinuosity results from this experiment compared with the experiment with one inclined plate. A comparison might lead to conclusions about the surface tension influence. Moreover, for both experiments it is interesting to derive whether these planform shapes represent a state in which the entropy production is minimal.

The principle of minimal entropy production can be used not only for meandering channels, but also for many other problems. Especially for complex problems, where solution of the momentum equations is difficult, the minimization theory can be useful. For example, it was already applied to find the drainage pattern found in nature, for the derivation of the three dimensional long structure and the branching pattern of trees.

Bibliography

S.-J. van Andel. Uniform energy dissipation explaining typical planform of river meander bend. M.Sc. thesis, Wageningen Univ., 2002.

R.A. Bagnold. Some aspects of the shape of river meanders. *U.S. Geol. Surv. Prof. Paper.*, 282-E, 1960.

Z.B. Begin. Stream curvature and bank erosion: A model based on the momentum equation. *J. Geol.*, 89:497–504, 1981.

R.B. Bird, W.E. Stewart, and E.N. Lightfoot. *Transport phenomena.* Wiley, New York, 1960.

K.A. Bowker. Albert einstein and meandering rivers. *Earth Sci. Hist.*, 1(1), 1988.

A. E. Bryson jr. and Y. Ho. *Applied optimal control: optimization, estimation and control.* Hemisphere publishing corporation Univ. Press, New York, 1975.

M.M. de las Heras Cadallero. *On variational data assimlation in ocean wave models.* Ph.d. thesis, University of Utrecht, 1994.

R.F. I Carcho and R.V. Sol. Optimization in complex networks, 2002. URL `http://complex.upf.es`.

M.A. Carson and M.F. Lapointe. The inherent asymmetry of river meander planform. *J. Geol.*, 91:41–55, 1983.

H.H. Chang. Analysis of river meanders. *J. Hydraul. Eng. ASCE*, 110(1):37–50, 1984.

A. Clebsch. unknown, 1859.

J.B. Culkin and S.H. Davis. Meandering of water rivulets. *A.I.Ch.E. J.*, 30(2): 263–267, 1984.

B.W. Davy and T.R.H. Davies. Entropy concepts in fluvial geomorphology: A reevalution. *Water Resour. Res.*, 15(1):103–106, 1979.

J.F. Douglas, J.M. Gasiorek, and J.A. Swaffield. *Fluid mechanics.* Addison Wesley Longman Ltd., Edinburgh, 1985.

B.F. Edwards and D.H. Smith. River meandering dynamics. *Phys. Rev. E*, 65, 2002. doi:10.1103/PhysRevE.65.046303.

R.I. Ferguson. Regular meander path models. *Water Resour. Res.*, 9(5):1079–1086, 1973.

R.I. Ferguson. Meander irregularity and wavelength estimation. *J. Hydrol.*, 26: 315–333, 1975.

G.R. Fowles and G.L. Cassiday. *Analytical mechanics.* Saunders college publishing, New York, 1999.

P. Glansdorff and I. Prigogine. On a general evolution criterion in macroscopic physics. *Physica*, 30:351–374, 1964.

J.W. Harris and H. Stocker. *Handbook of mathematical and computational science.* Springer, New York, 1998.

K.C. Heidorn. A jet stream runs through it, 2002. URL http://www.suite101.com/article.cfm/13646/96006.

H. Helmholtz. unknown. *Verh. Naturhist.-med. Ver.*, 1:223, 1868.

R.D. Hey. Geometry of river meanders. *Nature*, 262:482–484, 1976.

J. Hooke. River meander behavior and instability: a framework for analyis. *Trans. Inst. Br. Geogr.*, 28(2):238–253, 2003.

J.M. Hooke. Cutoffs galore!: occurence and causes of multiple cutoffs on a meandering river. *Geomorphology*, 2004.

R. le B. Hooke. Distribution of sediment transport and shear stress in a meander bend. *J. Geol.*, 83(5):543–565, 1975.

A.D. Howard and T.R. Knutson. Sufficient conditions for river meandering: a simulation approach. *Water Resour. Res.*, 20(11):1659–1667, 1984.

S. Ikeda, G. Parker, and K. Sawai. Bend theory of river meanders. Part 1. Linear development. *J. Fluid Mech.*, 112:363–377, 1981.

M.S.W. Jefferson. Limiting width of meander belts. *Natl. Geogr.*, pages 373–384, Oct. 1902.

H. Johannesson and G. Parker. Velocity redistribution in meandering rivers. *J. Hydraul. Eng. ASCE*, 115(8):1019–1039, 1989.

D. Knighton. *Fluvial form and processes: a new perspective.* University of Sheffield, United Kingdom, 1998.

G. Komatsu and V.R. Baker. Channels in the solar system. 44:801–815, 1996.

D.E. Lambregts. Numerieke oplossingen van optimale besturingsproblemen met toestandsbegrenzingen. M.Sc. thesis, Wageningen Univ., 1995.

S.T. Lancaster and R.L. Bras. A simple model of river meandering and its comparison to natural channels. *Hydrol. Process.*, 16:1–26, 2002. doi:10.1002/hyp.273.

W.B. Langbein and L.B. Leopold. River meanders - theory of minimum variance. *U.S. Geol. Surv. Prof. Paper.*, 422-H, 1966.

L.B. Leopold. *A view of the river.* Harvard Univ. Press, Cambridge, 1994.

L.B. Leopold and W.B. Langbein. River meanders. *Sci. Am.*, 214(6):60–70, 1966.

L.B. Leopold, M.G. Wolman, and J.P. Miller. *Fluvial processes in geomorpholgy.* Freeman and co., San Francisco, 1964.

T.B. Liverpool and S.F. Edwards. Dynamics of a meandering system. *Phys. Rev. E*, 75(16):3016–3019, 1995.

G.C. Nanson and J.C. Croke. A genetic classification of floodplains. *Geomorphology*, 4:459–486, 1992.

A.J. Odgaard. Meander flow model. I: Development. *J. Hydraul. Eng. ASCE*, 112(12):1117–1136, 1986a.

A.J. Odgaard. Meander flow model. II: Applications. *J. Hydraul. Eng. ASCE*, 112(12):1137–1150, 1986b.

A.J. Odgaard. Streambank erosion along two rivers in iowa. *Water Resour. Res.*, 23:1225–1236, 1987.

H.C. Ohanian. *Physics.* W.W. Norton, New York, 1989.

G. Parker and E.D. Andrews. On the time development of meander bends. *J. Fluid Mech.*, 162:139–156, 1986.

G. Parker, P. Diplas, and J. Akiyama. Meander bends of high amplitude. *J. Hydraul. Eng. ASCE*, 109(10):1323–1337, 1983.

G. Parker, K. Sawai, and S. Ikeda. Bend theory of river meanders. Part 2. Nonlinear deformation of finite-amplitude bends. *J. Fluid Mech.*, 115:303–314, 1982.

J.F. Pfaff. Eine allgemeine methode partielle differentialgleichungen zu integrieren. *Abh. kon. Akad. Wiss.*, 1815.

I. Prigogine. Etude thermodynamique des phenomenes irreversibles. *Bull. Cl. Acad. Roy. Belg.*, 31:600, 1945.

I. Prigogine and I. Stengers. *Order out of chaos: man's new dialogue with nature.* Fontana, London, 1985.

B. Reiser. Real processing (RP) I: The principle of minimal entropy production (PME) of irreversible thermodynamics and the principle of minimal deformation (PMD) of hydrodynamics, their dependence and applications. *Physica A*, 229:127–142, 1996.

B. Reiser. Real processing II: Extremal principles of irreversible thermodynamics, relations, generalizations and time dependence. *Physica A*, 253:223–246, 1998.

B. Reiser. Real processing III. The generalized statement of Helmholtz and Rayleigh and its meaning for process engineering. *Physica A*, 286:239–282, 2000.

B. Reiser. Real processing IV. The derivation of the Navier-Stokes equation from the principle of minimum deformation. *Physica A*, 291:512–522, 2001.

B. Reiser. Meander of rivers, 2003.

S.A. Schumm. Introductionary chapter. In S.A. Schumm and B.R. Winkley, editors, *The variabililty of large alluvial rivers.* ASCE press, New York, 1994.

S.A. Schumm, H.R. Khan, B.R. Winkley, and L.G. Robbins. Variability of river patterns. *Nature Phys. Sci.*, 237:75–76, 1972.

S.A. Schumm and R.W. Lichty. Time, space and causality in geomorphology. *J. of Science*, 263:110–119, 1965.

M. Shams, G. Ahmadi, and D.H. Smith. Computational modeling of flow and sediment transport and deposition in meandering rivers. *Adv. Water Resour.*, 25:689–699, 2002.

A.M.A.F. da Silva. Friction factor of meandering flows. *J. Hydraul. Eng. ASCE*, 125(7):779–783, 1999.

J.D. Smith and S.R. McLean. A model for flow in meandering streams. *Water Resour. Res.*, 20(9):1301–1315, 1984.

H.-H. Stølum. River meandering as a self-organization process. *Science*, 271: 1710–1713, 1996.

H.-H. Stølum. Planform geometry and dynamics of meandering rivers. *Geol. Soc. Am. Bull.*, 110(11):1485–1498, 1998.

A.J. Teuling. Entropy and river meander planform. M.Sc. thesis, Wageningen Univ., 2002.

J.J. Oter Vives. Study on the meandering equilibrium planform equations: validity under different flow model assumptions. M.Sc. thesis, Wageningen Univ., 2003.

J. Vlassenbroeck and R. van Dooren. A chebyshev technique for solving non-linear optimal control problems. *Transaction on automatic control*, 33(4): 333–340, 1988.

S.E. Vos. *Variational wave data-assimilation for operational wave forecasting.* Ph.d. thesis, TU Delft, 2002.

L.G. van Willigenburg. Systems and control theory part 2: optimal control, 2003.

H.P. Wolfert. *Geomorphological change and river rehabilitation: case studies on lowland fluvial systems in the Netherlands.* Ph.d. thesis, Utrecht Univ., 2001.

C.R. Wylie and L.C. Barrett. *Advanced engineering mathematics.* McGraw-Hill Kogakusha, United States, 1982.

C.T. Yang. Force, energy, entropy, and energy dissipation rate. In V.P. Singh and M. Fiorentino, editors, *Entropy and energy dissipation in water resources.* Kluwer, Dordrecht, 1992.

C.T. Yang and C.C.S. Song. Theory of minimum rate of energy dissipation. *J. Hydraul. Div. ASCE*, 105(HY7):769–784, 1979.